Characterization of a C3 deoxygenation pathway reveals a key branch point in aminoglycoside biosynthesis

Meinan Lv, Xinjian Ji, Junfeng Zhao, Yongzhen Li, Chen Zhang, Li Su, Wei Ding, Zixin Deng, Yi Yu and Qi Zhang

Supplementary Methods

Instrumentation

High-performance liquid chromatography (HPLC) was performed using a Thermo Scientific Dionex Ultimate 3000 system with an evaporative light scattering detector (Alltech, 2000ES) equipped with a DIKMA Diamonsil C18 column (3.5 μm，150×2.1 mm). High resolution mass spectra (HRMS) were acquired using a Q-Exactive™ Focus Hybrid Quadrupole-Orbitrap Mass Spectrometer (Thermo Fisher Scientific Inc.) equipped with a Dionex Ultimate 3000 HPLC system (Thermo Fisher), or an LTQ XL Orbitrap Mass Spectrometer equipped with an Accela 600 U-HPLC system (Thermo Fisher Scientific Inc.), or a Synapt ESI quadrupole ToF Mass Spectrometry System (Waters) equipped with an Acquity Ultra Performance Liquid Chromatography (UPLC) system (Waters). NMR spectra were recorded using Varian Inova 500 MHz NMR spectrometer. UV-vis spectroscopy analysis was performed on a 1900 double beam UV-vis spectrometer (Yoke Instrument Co. Ltd., Shanghai, China). EPR spectra were obtained at X-band using a Bruker EMX plus 10/12 spectrometer system, equipped with an Oxford ESR910 liquid helium continuous flow cryostat (Oxford Instrument Co.). PCR was performed on a Bio-Rad T100^{TM} Thermal Cycler using Phanta Max Super-Fidelity DNA Polymerase (Vazyme Biotech) or KOD DNA polymerase (TOYOBO).

Chemicals and biochemicals

All chemical reagents and anhydrous solvents were purchased from commercial sources and used without further purification unless otherwise specified. S-adenosyl-L-methionine (SAM), thiostrepton, paromycin, neomycin, tobramycin, and spectinomycin were purchased from Sangon

Biotech Co. Ltd (Shanghai, China). Lividomycin was purchased from Biolise Co. Ltd (Xiamen, China). $Fe(NH_4)_2(SO_4)_2 \cdot 6H_2O$ and Na_2S were from Sigma-Aldrich Co. Ltd (USA). Kanamycin and culture media were from Sinopharm Chemical Reagent Co. Ltd (China). Gentimicin X2, gentimicin G418, and the GenQ expressing plasmid pET28/VM_GenQ are precious gifts from Prof. Yuhui Sun (Wuhan University).[1] Enzymes were from Takara Biotechnology (Dalian, China) or from Vazyme Biotech (Nanjing, China) unless otherwise specified. Primers were synthesized at Invitrogen Biotech Co. Ltd (Shanghai, China).

DNA sequencing and analysis

S. tenebrarius genomic DNA was prepared using UltraClean Microbial DNA Isolation Kit (Anbiosci Ltd, Shenzhen, China), and was then sequenced by Illumina Hiseq 2000 with a 300 bp paired-end library through TruSeq method at GenScript Co. Ltd (Nanjing, China). A total of 3,685,798 paired-reads were obtained and assembled by using the assembly programs SOAPdeNOVO[2] with the parameters "sequence length > 25 bp and base quality > 20". When the K-mer was 21, the best assembly result could be obtained. The resultant 384 contigs were further annotated by RAST (http://rast.nmpdr.org/rast.cgi).

Construction of the plasmids for genetic manipulation of *Streptomyces tenebrarius*

Because the apramycin producer *Streptomyces tenebrarius* is resistant to apramycin, in this study we constructed two plasmids containing a spectinomycin resistance gene *aadA* for genetic manipulation of *S. tenebrarius*. *aadA* was amplified by PCR using a primer pair aadA-F and aadA-R (**Supplementary Table 2**), and the plasmid pIJ778[3] as the template. The ~1.1 kb DNA fragment containing *aadA* and its promoter region was digested by SacI, and recovered using a Qiagen PCR purification kit. This DNA fragment was ligated with a ~2.7 kb fragment obtained by SacI digestion of pOJ260,[4] or a ~5.2 kb fragment obtained by SacI digestion of pIB139,[5] using T4 DNA ligase (Takara Biotechnology). Chemically competent *E. coli* DH5α cells were transformed with the ligation mixture and plated on LB-agar containing spectinomycin (50 μg/mL)

to screen for positive clones. Clones were confirmed by DNA sequencing at Genewiz Co. Ltd (Suzhou, China). The resulting plasmids pWHU258 (pOJ260 derivative) and pWHU268 (pIB139 derivative) were used for gene-knockout and complementation experiments, respectively.

Construction of the Δ*aprD4* mutant

To inactivate *aprD4*, a 2241 bp upstream fragment and 2400 bp downstream fragment were amplified separately from the *S. tenebrarius* genomic DNA by PCR using the primer pair aprD4-Left-F and aprD4-Left-R, and the pair aprD4-Right-F and aprD4-Right-R, respectively (**Supplementary Table 2**). The resulting fragments were purified using a Qiagen PCR purification kit, and then cloned into the HindIII/EcoRI site of pWHU258 using In-fusion HD Cloning Kit (Clontech) to give the in-frame deletion construct pWHU288. pWHU288 was then transferred into *S. tenebrarius* via *E. coli-Streptomyces* conjugation. The *aprD4* in-frame deletion mutant (designated as WDY288) was screened and its genotype was confirmed by PCR and DNA sequencing, and by Southern blot (Figure S1).

Construction of the Δ*aprD3* mutant

To inactivate *aprD3*, a 2265 bp upstream fragment and 2289 bp downstream fragment were amplified separately from the *S. tenebrarius* genomic DNA by PCR using the primer pair aprD3-Left-F and aprD3-Left-R, and the pair aprD3-Right-F and aprD3-Right-R, respectively (**Supplementary Table 2**). The resulting fragments were purified using a Qiagen PCR purification kit, and then cloned into the HindIII/EcoRI site of pWHU258 using In-fusion HD Cloning Kit (Clontech) to give the in-frame deletion construct pWHU289. pWHU289 was then transferred into *S. tenebrarius* via *E. coli-Streptomyces* conjugation. The *aprD3* in-frame deletion mutant (designated as WDY289) was screened and its genotype was confirmed by PCR and DNA sequencing, and by Southern blot (Figure S12)

Construction of the Δ*aprQ* mutant

To inactivate *aprQ*, a 2217 bp upstream fragment and 2232 bp downstream fragment were amplified separately from the *S. tenebrarius* genomic DNA by PCR using the primer pair aprQ-Left-F and aprQ-Left-R, and the pair aprQ-Right-F and aprQ-Right-R, respectively (**Supplementary Table 2**). The resulting fragments were purified using a Qiagen PCR purification kit, and then cloned into the HindIII/EcoRI site of pWHU258 using In-fusion HD Cloning Kit (Clontech) to give the in-frame deletion construct pWHU290. pWHU290 was then transferred into *S. tenebrarius* via *E. coli*-*Streptomyces* conjugation. The *aprQ* in-frame deletion mutant (designated as WDY290) was screened and its genotype was confirmed by PCR and DNA sequencing, and by Southern blot (Figure S20)

Construction of the Δ*tobQ* mutant

To inactivate *tobQ*, a 2213 bp upstream fragment and 2135 bp downstream fragment were amplified separately from the *S. tenebrarius* genomic DNA by PCR using the primer pair tobQ-Left-F and tobQ-Left-R, and the pair tobQ-Right-F and tobQ-Right-R, respectively (**Supplementary Table 2**). The resulting fragments were purified using a Qiagen PCR purification kit, and then cloned into the HindIII/EcoRI site of pWHU258 using In-fusion HD Cloning Kit (Clontech) to give the in-frame deletion construct pWHU291. Plasmid pWHU291 was then transferred into *S. tenebrarius* via *E. coli*-*Streptomyces* conjugation. The *tobQ* in-frame deletion mutant (designated as WDY291) was screened and its genotype was confirmed by PCR and DNA sequencing.

Construction of the Δ*aprQ*Δ*tobQ* double knockout mutant

To obtain Δ*aprQ*Δ*tobQ* double in-frame deletion mutant, the *tobQ* in-frame deletion construct pWHU191 was transferred into the Δ*aprQ* mutant WDY290 via *E. coli*-*Streptomyces* conjugation. The Δ*aprQ*Δ*tobQ* double in-frame deletion mutant (designated as WDY292) was screened and its genotype was confirmed by PCR and DNA sequencing, and by Southern blot (Figure S21).

Construction of the Δ*aprD4*Δ*aprQ* mutant

To obtain Δ*aprD4*Δ*aprQ* double in-frame deletion mutant, a 2248 bp upstream fragment and a 2400 bp downstream fragment were amplified separately from the *ΔaprQ* mutant WDY290 genomic DNA by PCR using the primer pair aprD4aprQ-F and aprD4-Left-R, and the pair aprD4-Right-F and aprD4-Right-R, respectively (Supplementary Table 2). The resulting fragments were purified using a Qiagen PCR purification kit, and then cloned into the HindIII/EcoRI site of pWHU258 using In-fusion HD Cloning Kit (Clontech) to give the in-frame deletion construct pWHU293. Plasmid pWHU293 was then transferred into the Δ*aprQ* mutant WDY290 via *E. coli-Streptomyces* conjugation. The Δ*aprD4*Δ*aprQ* double in-frame deletion mutant (designated as WDY293) was screened and its genotype was confirmed by PCR and DNA sequencing, and by Southern blot (Figure S23).

Construction of the Δ*aprD4*Δ*tobQ* mutant

To obtain Δ*aprD4*Δ*tobQ* double in-frame deletion mutant, the *tobQ* in-frame deletion construct pWHU291 was then transferred into the Δ*aprD4* mutant WDY288 via *E. coli-Streptomyces* conjugation. The Δ*aprD4*Δ*tobQ* double in-frame deletion mutant (designated as WDY294) was screened and its genotype was confirmed by PCR and DNA sequencing, and by Southern blot (Figure S22).

Southern blot analysis

Genomic DNAs of *S. tenebrarius* wild type and mutant strains were prepared according to the standard protocol[6]. DNA samples were digested with appropriate restriction enzymes, separated by electrophoresis on agarose gels, and blotted on Hybond-N^+ positive-charged nylon membranes (Roche). Hybridization was carried out according to the manufacturer's instruction (Roche) by using probes labeled with digoxigenin-11-dUTP (Roche).

Complementation of the gene-knockout mutants

The complementation plasmids were prepared by cloning *aprD4* (PCR using a primer pair HB-aprD4-F and HB-aprD4-R), *aprD3* (PCR using a primer pair HB-aprD3-F and HB-aprD3-R), AprQ (PCR using a primer pair HB-aprQ-F and HB-aprQ-R), and *tobQ* (PCR using a primer pair HB-tobQ-F and HB-tobQ-R) into the NdeI/EcoRI site of pWHU268 to result in pWHU300, pWHU301, pWH302, pWHU303 for complementation of *aprD4*, *aprD3*, *aprQ, tobQ*, respectively (**Figure S 2-3**). These pWHU268 derivative plasmids, which can be integrated into the *attB* site in *Streptomyces* chromosome via phage ΦC31 integrase-catalyzed site-specific recombination,[7,8] were each transferred into a gene knockout mutant via *E. coli-Streptomyces* conjugation to give WDY300 (Δ*aprD4* complementation by *aprD4*), WDY301 (Δ*aprD3* complementation by *aprD3*), WDY302 (Δ*aprQ* complementation by *aprQ*), WDY303 (Δ*tobQ* complementation by *tobQ*), WDY306 (Δ*aprQ*Δ*tobQ* complementation by *aprQ*), WDY307 (Δ*aprD4*Δ*aprQ* complementation by *aprQ*), and WDY308 (Δ*aprD4*Δ*aprQ* complementation by *tobQ*).

In vivo production of aminoglycosides and their biosynthetic intermediates

SPA medium (in grams per liter of solution: soluble starch, 20; beaf extract, 1; $MgSO_4$, 0.5; KNO_3, 1; NaCl, 0.5; K_2HPO_4, 0.5; agar, 20) was used for spore production. The spore suspension of *S. tenebrarius* and the related mutants were inoculated into 5ml TSBY medium (in grams per liter of solution: trypticase soy broth, 30.0 g; yeast extract, 3.0; NaCl 13.0g; $MgCl_2$•$6H_2O$, 4.0g; $MgSO_4$•7H2O, 3.45g; KCl, 0.34g; $CaCl_2$•$2H_2O$, 0.14g; the pH was adjusted to 7.2 before autoclave at 120 ^oC for 15 min). The culture was grown at 37 °C and 220 *rpm* for 36 h and was used to inoculate 50ml SPC fermentation medium containing the followings (in grams per liter of solution): glucose, 40; peptone, 10; soybean meal, 4; corn meal, 10; $MgSO_4$•$7H_2O$, 4; NH_4Cl, 5; $FeSO_4$, 0.5; $MnCl_2$, 0.3; $ZnSO_4$, 0.03; $CaCO_3$, 5. The cells were grown at 37 °C and 220 *rpm* for 7 days, and the culture supernatant was collected by centrifugation at 5000 rpm for 15 min, and was adjusted to a pH of 2 ~ 3 with oxalate. After removal of the insoluble fraction by centrifugation at 5000 rpm for 30 min, the solution was passed through a column containing 5 ml 732 cation exchange resin (Hebi Juxing Resinco., Ltd, Hebi, China). The column was then washed with 50 mL of distilled water followed by 10 mL 3% ammonia hydroxide solution. The eluate was purged

with a nitrogen stream and then taken to dryness by lyophilization. The residue was dissolved in 500 μL of methanol before HPLC and LCMS analysis.

Isolation and structure characterization of oxyapramycin, lividamine, and paromamine

Oxyapramycin and paromamine were isolated from the fermentation culture of the Δ*aprD4* mutant WDY288, and lividamine was isolated from the fermentation culture of the Δ*aprQ* mutant WDY290. The culture supernatant was adjusted to a pH of 2 ~ 3 with oxalate and the insoluble fraction was removed by centrifugation (5000 rpm, 30 min). The supernatant was extracted by the crude 732 cation exchange resin. The resulting resin was packed on a column, washed by distilled water and then by 3% ammonia hydroxide solution. The ammonia hydroxide eluate was then passed through an 801 anion-exchange column, and the eluate was purged with a nitrogen stream and then taken to dryness by lyophilization. The lyophilized residue was then separated by semi-preparative HPLC using a DIONEX System equipped with UltiMate 3000 Pump connecting with Evaporative Light Scattering Detector (Alltech, 2000ES) with an Agilent ZORBAX SB-C18 column (5 μm, 9.4×250 mm). The column was equilibrated with 80% solvent A (H_2O, 10 mM heptafluorobutyric acid) and 20% solvent B (CH_3CN), and developed at a flow rate of 3 ml/min: 0-3 min, constant 80%A/20%B; 3-5 min, a linear gradient to 75%A/25%B; 5-9 min, a linear gradient to 71%A/29% B; 9-15 min, a linear gradient to 65%A/35%B, 15-20 min, a linear gradient to 62%A/38% B; 20-30 min, a linear gradient to 80%A/20%B.

Construction of plasmids for overexpressing N-terminally hexa-His-tagged AprD3 and AprD4

The *aprD3* and *aprD4* genes were amplified from the *S. tenebrarius* genomic DNA using a primer pair N-AprD3-F and N-AprD3-R, and a pair N-AprD4-F and N-AprD4-R (Table S1), respectively. The PCR amplified products were digested with NcoI and XhoI, purified using a Qiagen PCR purification kit, and inserted into the same restriction site of the expression vector pET28a (Novagen). Chemically competent *E. coli* DH5α cells were transformed with the ligation mixture

and plated on LB-agar containing kanamycin (50 μg mL-1) to screen for positive clones, which were confirmed by DNA sequencing.

Construction of the plasmid for overexpressing N-terminally Flag-tagged AprD3

The *aprD3* gene was amplified from the *S. tenebrarius* genomic DNA using a primer pair N-flag-AprD3-F and N-AprD3-R (table S2) carrying an engineered Flag tag. The PCR amplified products were digested with NcoI and XhoI, purified using a Qiagen PCR purification kit, and inserted into the same restriction site of the expression vector pET28a (Novagen). Chemically competent *E. coli* DH5α cells were transformed with the ligation mixture and plated on LB-agar containing kanamycin (50 μg/mL) to screen for positive clones, which were confirmed by DNA sequencing.

AprD4 mutagenesis

To reveal the [4Fe-4S] cluster binding site of AprD4, all 12 Cys residues in AprD4 were individually replaced by an Ala residue, and this was achieved by using a site-directed mutagenesis procedure reported previously.[9] PCR was performed with each primer pair (e.g. AprD4-C203A-F and AprD4-C203A-R for producing AprD4 C203A, etc., the primer sequences are listed in **Supplementary Table 2**), and the AprD4-expressing plasmid as the template. After checking the PCR products by agarose gel electrophoresis, 1 μL of the PCR product was treated with the restriction enzyme DpnI (TOYOBO), and the total 20 μL reaction solution was incubated at 37 ^{o}C for ～1.5 h. 2.5 μL of the resulting solution was used for transformation of *E. coli* DH10B cells. The positive clones were picked and verified by DNA sequencing.

Protein Expression

E. coli BL21 (DE3) cells were transformed via electroporation with the expression plasmids. A single colony transformant was used to inoculate a 5 mL culture of LB supplemented with 100 μg/mL kanamycin. The culture was grown at 37 °C for 12 h and was used to inoculate 1 L of LB

medium containing 100 μg/mL kanamycin. Cells were grown at 37 °C and 220 rpm to an OD_{600}～0.6-0.8, and then IPTG was added to a final concentration of 0.1 mM. To express AprD4 wild type and mutant enzymes, sterilized $Fe(NH_4)_2(SO_4)_2$ solution was added to the culture to a final concentration of 10 μM. After additional 8 h of incubation, the cells were harvested by centrifugation at 5000 rpm for 15 min at 4 °C. The pellet was used directly for protein purification or stored at −80 °C before use.

Purification of AprD3 and GenQ

AprD3 and GenQ were purified aerobically. The cell pellet collected by centrifugation was re-suspended in 20 ml lysis buffer (50 mM MOPS, 200 mM NaCl, and 10% glycerol, pH 8.0), and was lysed by a high pressure homogenizer (FB-110X, Shanghai Litu Mechanical Equipment Engineering Co., Ltd, China). Cell debris was removed via centrifugation at 14000 rpm for 30 min at 4 °C. The supernatant was incubated with 4 ml Ni-NTA resin pre-equilibrated with the lysis buffer, and then subjected to affinity purification on a column. The desired elution fractions were combined and concentrated using an Amicon Ultra-15 Centrifugal Filter Unit, and the concentrated protein solution was desalted using a DG-10 column (Bio-Rad) pre-equilibrated with the elution buffer (50 mM MOPS, 25 mM NaCl, and 10% (v/v) glycerol, pH 8.0). The protein fraction was collected and concentrated, analyzed by SDS-PAGE (10% Tris-glycine gel), and was used directly for in vitro assay or stored at −80 °C upon further use. Protein concentration was determined using a Bradford assay kit (Promega) using bovine serum albumin (BSA) as a standard.

Preparation of the reconstituted AprD4 wild type and mutant enzymes

Purification and [4Fe-4S] reconstitution of AprD4 wild type and mutant enzymes were performed in an anaerobic glove box (Coy Laboratory Product Inc., USA) with less than 2 ppm of O_2. The cell pellet was resuspended in 20 ml of the lysis buffer (50 mM MOPS, 200 mM NaCl, and 10% glycerol, pH 8.0), and was lysed by sonication on ice. Cell debris was removed via centrifugation at 14000 rpm for 30 min at 4 °C. The supernatant was incubated with 4 ml Ni-NTA resin pre-equilibrated with the lysis buffer, and then subjected to affinity purification on a column. The

desired fractions were combined and concentrated using an Amicon Ultra-15 Centrifugal Filter Unit, and analyzed by SDS-PAGE (12% Tris-glycine gel). Protein concentration was determined using a Bradford assay kit (Promega) using BSA as a standard.

Native-PAGE analysis

Native-PAGE analysis of AprD4 and AprD3 mixtures, which were incubated anaerobically at room temperature for 30 min or 2 h, was carried out with a 12% Tris-glycine gel. SDS was omitted in the analysis and the electrophoresis was performed at 4 °C.

Western blot

SDS-PAGE analysis was run in a 12% gel for ~2 h at 120 V. Proteins were transferred from the gel to a PVDF membrane; the latter was then cut into two parts from a line roughly around 40 kDa, allowing separation of AprD3 and AprD4 into two PVDF membranes. The membranes were incubated in a PBS blocking buffer containing 5% skim milk at 4°C overnight, and were washed twice with PBST buffer (NaCl 8 g/L, KCl 0.2 g/L, $Na_2HPO_4 \cdot 12H_2O$, 3.58 g/L KH_2PO_4, 0.24 g/L, 0.05% tween). 1:2500 anti-Flag tag or anti-His tag mouse monocolonal antibodies were used to probe AprD3 and AprD4, respectively, and proteins were visualized by chemiluminescence by using 1:5000 IPKine HRP (Abbkine) and goat anti-mouse IgG fc secondary antibody (Abbkine, for AprD3) or goat anti-mouse igG LCS antibody (Abbkine, for AprD4).

Construction of pWDYHS01 for expressing proteins in *Streptomyces*

A 179 bp fragment containing an N-terminal His_6-tag and multiple cloning sites were amplified from pET28a by PCR using the primer pair pGM1190_F and pGM1190_R (**Supplementary Table 2**). PCR was carried out in 20 μL of volume with 5% DMSO and KOD DNA polymerase (TOYOBO), and the resulting fragments were cloned into pGM1190[10] by using an In-fusion HD Cloning Kit (Clontech) to yield the plasmid pWDYHS01 for protein expression in *Streptomyces*.

Construction of the *aprQ*-expressing *Streptomyces* strain WDY320

The gene *aprQ* was amplified by high fidelity PCR from *S. tenebrarius* genomic DNA using oligonucleotide primer pair N-AprQ-F and N-AprQ-R (**Supplementary Table 2**) carrying the engineered NdeI and XhoI restriction sites. The PCR-amplified gene product was purified, digested with NdeI and XhoI, and ligated into the NdeI/XhoI cleaved expression vector pWDYHS01 to generate pWHU320. pWHU320 was then transferred into *Streptomyces lividans* TK24. The resulting colonies were selected by *aac(3)IV* resistance marker and confirmed by PCR to obtain the recombinant strain WDY320.

Construction of the *tobQ*-expressing *Streptomyces* strain WDY321

tobQ was amplified by high fidelity PCR from *S. tenebrarius* genomic DNA using oligonucleotide primer pair N-TobQ-F and N-TobQ-R (**Supplementary Table 2**) carrying the engineered NdeI and XhoI restriction sites. The PCR-amplified product was purified, digested with NdeI and XhoI, and ligated into the NdeI/XhoI cleaved expression vector pWDYHS01 to yield pWHU321. pWHU321 was then transferred into *Streptomyces lividance* TK24, and the resulting colonies were selected by *aac(3)IV* resistance marker and confirmed by PCR to obtain the recombinant strain WDY321.

Phylogenetic analysis

The protein sequences in this study were obtained from the GenBank database; their accession numbers and the source organisms are listed in **Supplementary Table 1**. The sequences were aligned in ClustalX[11] using default parameters with iteration at each alignment step, and the alignments were manually fine-tuned afterwards. Bayesian inference was used to calculate posterior probability of clades utilizing the program MrBayes (version 3.2).[12] Final analyses consisted of two sets of eight chains each (one cold and seven heated), run for about 1 million generations with trees saved and parameters sampled every 100 generations. Analyses were run to reach a convergence with standard deviation of split frequencies <0.008. Posterior probabilities

were averaged over the final 75% of trees (25% burn in). The analysis utilized a mixed amino acid model with a proportion of sites designated invariant, and rate variation among sites modeled after a gamma distribution divided into eight categories, with all variable parameters estimated by the program based on BioNJ starting trees. The figures of the Bayesian phylograms were prepared by using Tree-View.[13]

Figure S1. In-frame deletion of *aprD4* in *S. tenebrarius*, showing the schematic representation of the in-frame deletion and the southern blot analysis. The probe is shown as a purple bar, and the arrows beside the southern blot data indicate the size of the expected signal fragments.

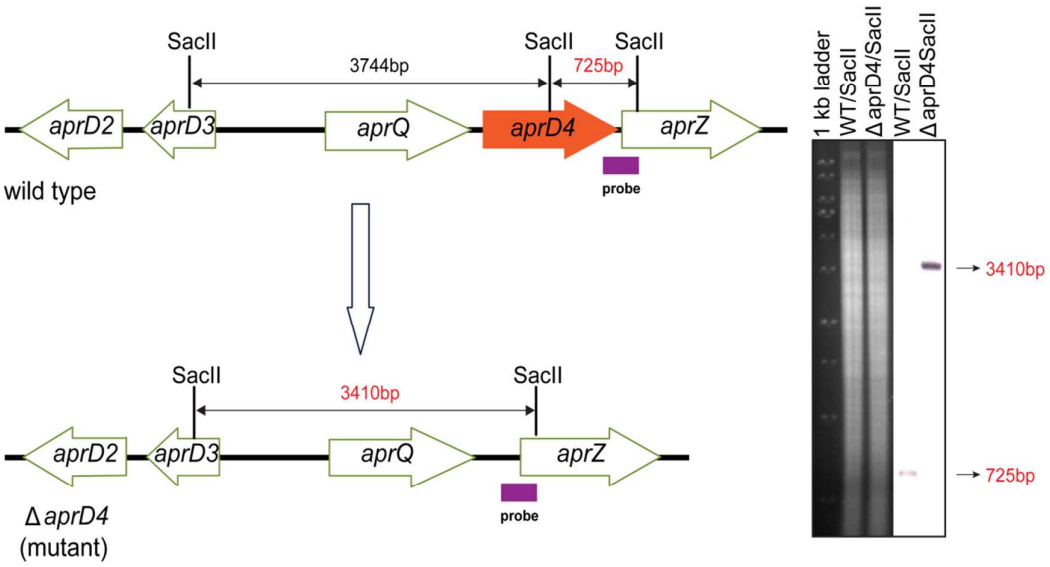

Figure S2. HR-MS/MS analysis of oxyapramycin purified from the fermentation culture of the Δ*aprD4* mutant, showing (A) the collision induced dissociation (CID) fragments, and (B) the MS/MS spectrum.

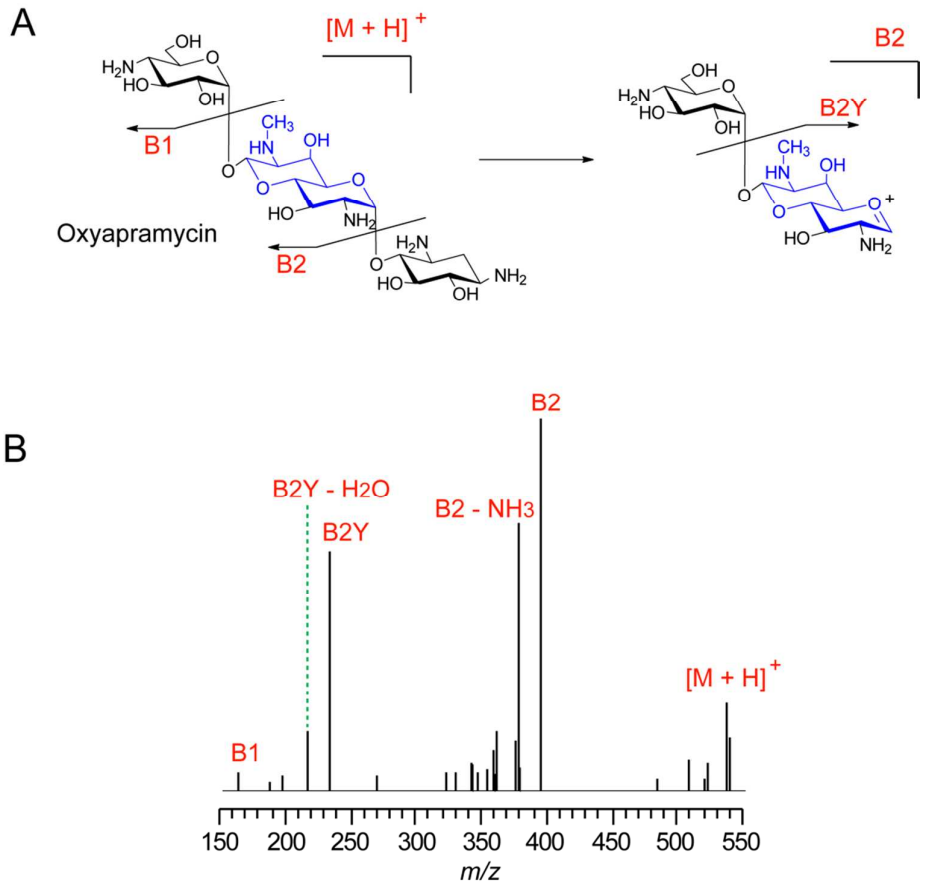

Figure S3. ^{1}H NMR analysis of oxyapramycin purified from the fermentation culture of the Δ*aprD4* mutant, showing (A) the chemical structure of oxyapramycin, and (B) the ^{1}H NMR spectrum.

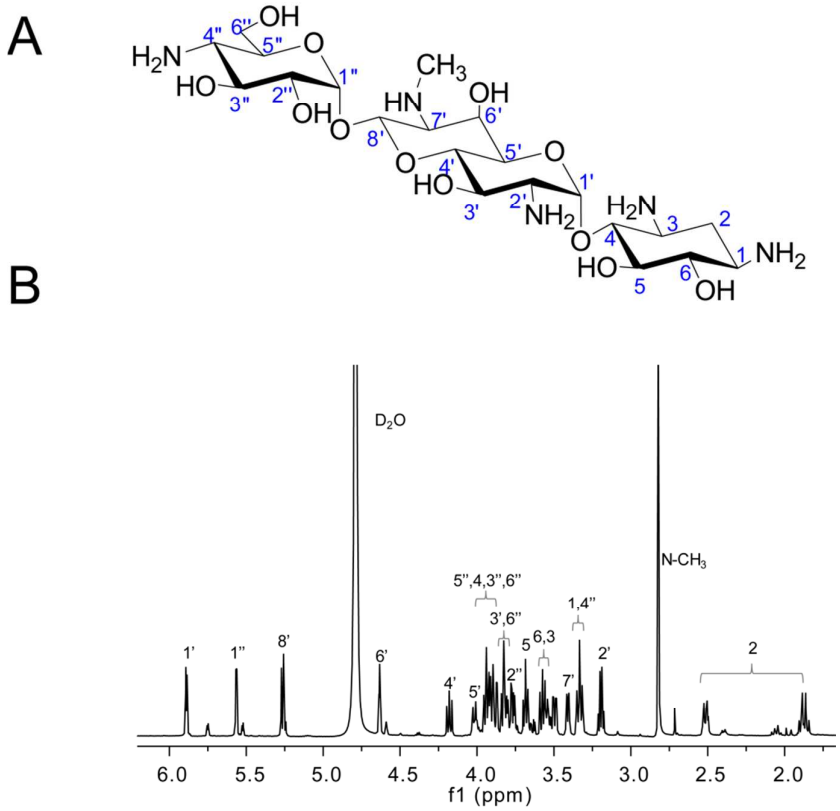

Figure S4. ^{13}C NMR analysis of oxyapramycin purified from the fermentation culture of the Δ*aprD4* mutant, showing (A) the chemical structure of oxyapramycin, and (B) the ^{13}C NMR spectrum.

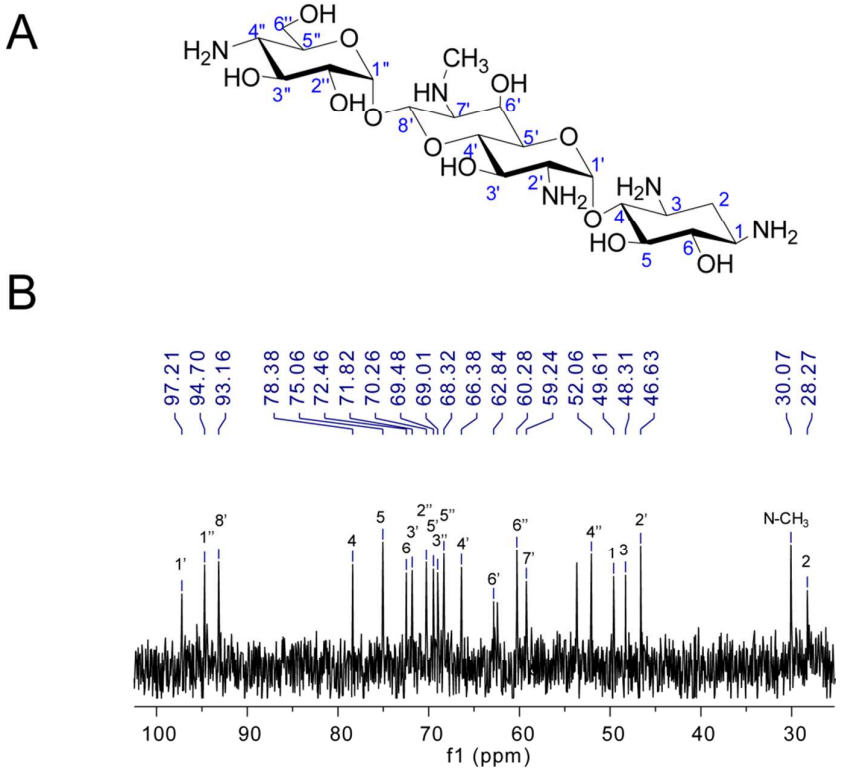

Figure S5. HR-MS/MS analysis of paromamine purified from the fermentation culture of the Δ*aprD4* mutant, showing (A) the collision induced dissociation (CID) fragments, and (B) the MS/MS spectrum.

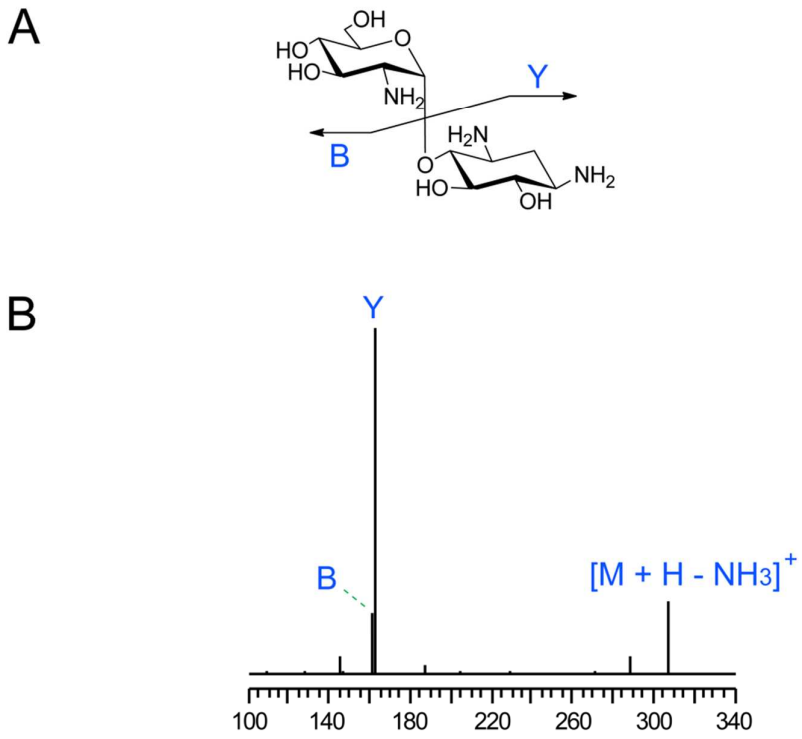

Figure S6. ^{1}H NMR analysis of paromamine purified from the fermentation culture of the Δ*aprD4* mutant, showing (A) the chemical structure of paromamine, and (B) the ^{1}H NMR spectrum.

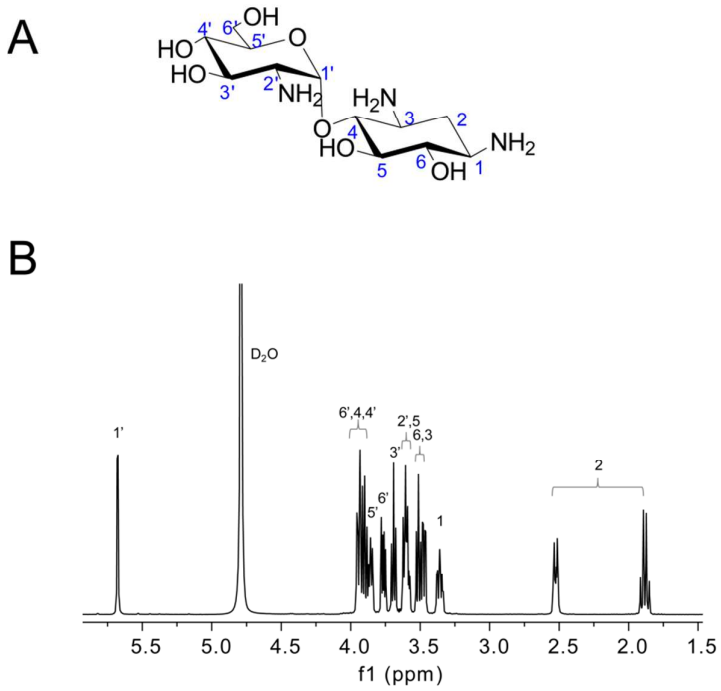

Figure S7. ^{13}C NMR analysis of paromamine purified from the fermentation culture of the Δ*aprD4* mutant, showing (A) the chemical structure of paromamine, and (B) the ^{13}C NMR spectrum.

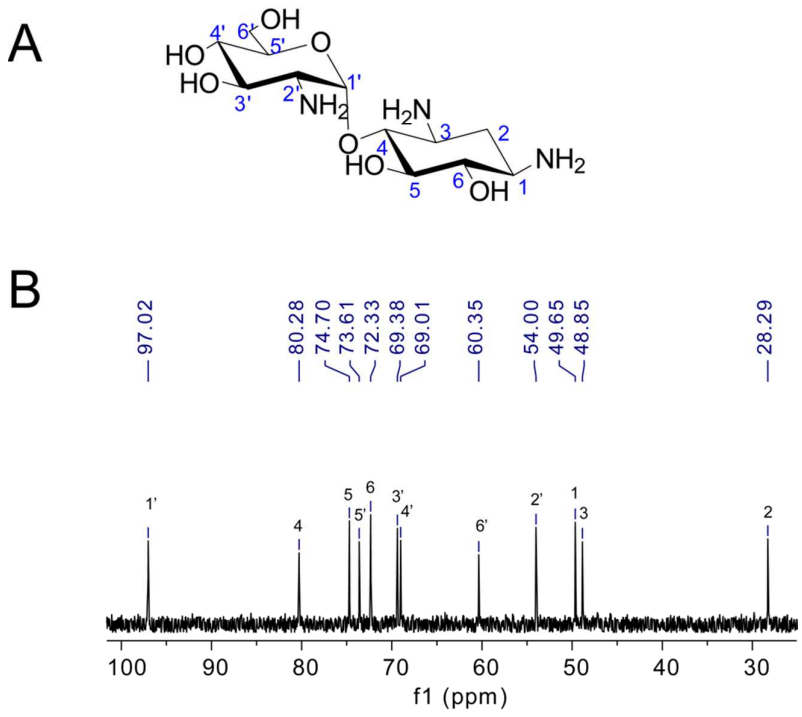

Figure S8. HPLC analysis of the SAM cleavage activity of the 12 AprD4 Cys-to-Ala mutants. The assays were performed by incubating 500 μM paromamine with ~40 μM reconstituted AprD4 mutant, 1 mM SAM and 4 mM sodium dithionite in 50 mM MOPS buffer (pH 8.0) at room temperature for ~3 h . Mutants with an intact CX_3CX_3C (**C**PYP**C**RFY**C**) motif all cleaved SAM with varied efficiencies, whereas the three mutants in which the CX_3CX_3C (**C**PYP**C**RFY**C**) motif was altered (shown in red bold font) had no detectable SAM cleavage activity. UV detector, 260 nm.

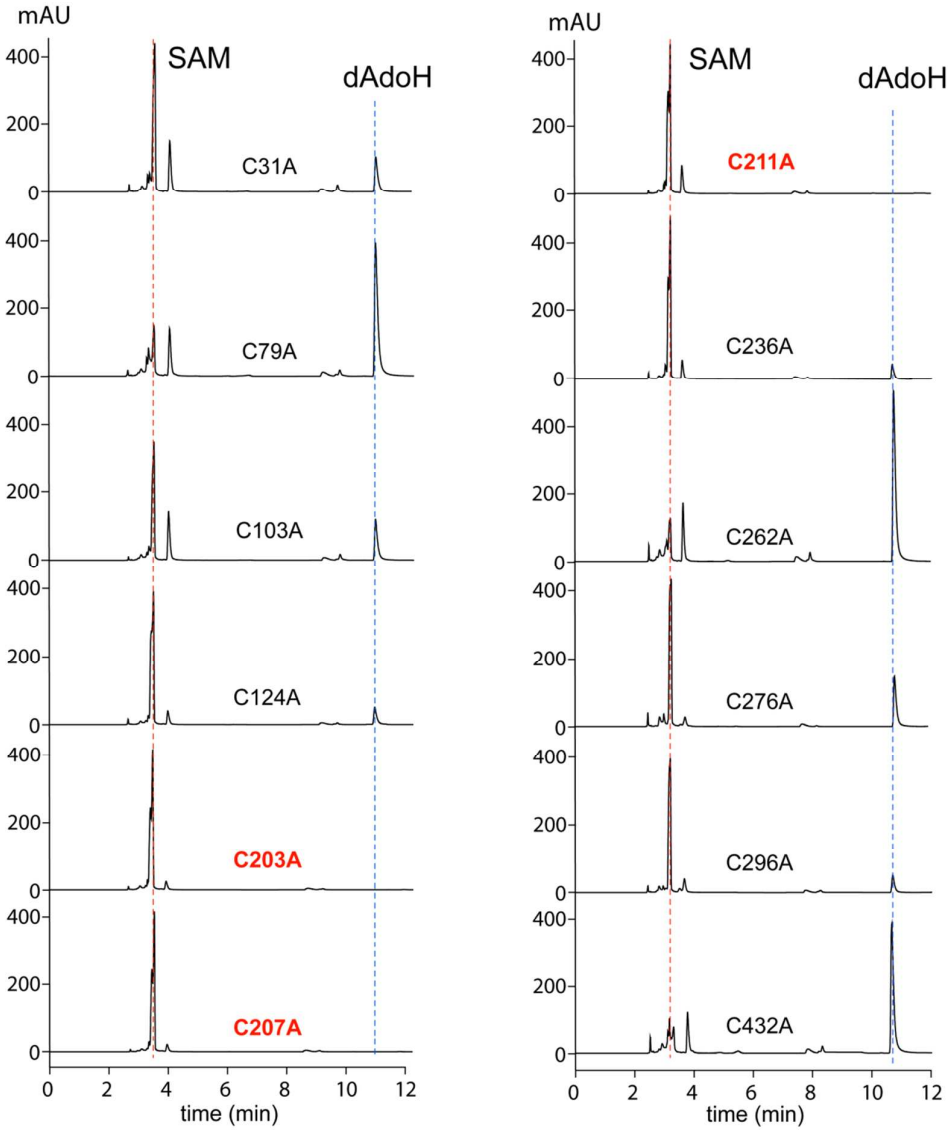

Figure S9. UV-vis spectra of the reconstituted AprD4 C207A mutant (red solid line) and the protein reduced with DTH (blue dashed line).

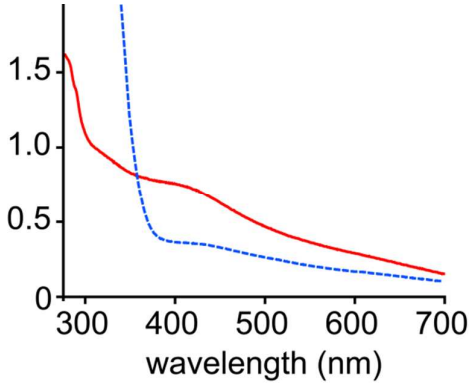

Figure S10. HR-MS/MS spectrum of DOP (**4**) and its ion fragments upon collision induced dissociation (CID).

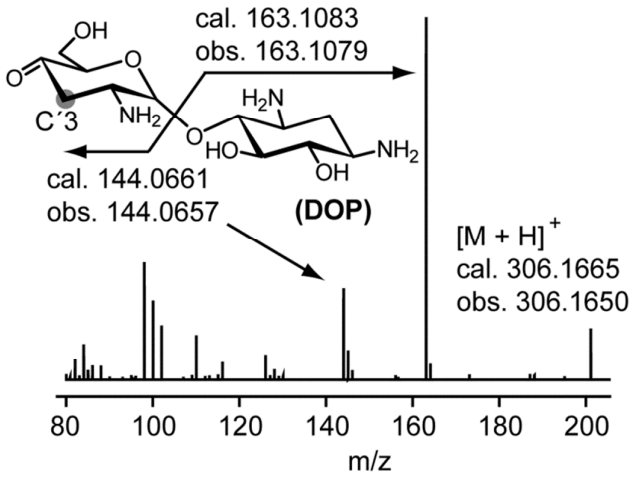

Figure S11. MS analysis of (A) dAdoH and (B) paromamine from AprD4-catalyzed reaction, which was performed in a buffer containing 67% D_2O and 100 μM paromamine, and incubated at room temperature for 5 h. Significant deuterium incorporation into paromamine was observed but deuterium incorporation into dAdoH was not apparent. (C) A hypothetic model for AprD4-catalzyed deuterium incorporation into paromamine. The substrate radical could abstract a deuterium atom from an unidentified source (e.g. a protein residue) or be reduced by DTH coupled with a deuterium transfer. Notably, similar observations of substrate deuteriation were also found in the study of the radical SAM enzymes DesII[14,15] and NosL[16].

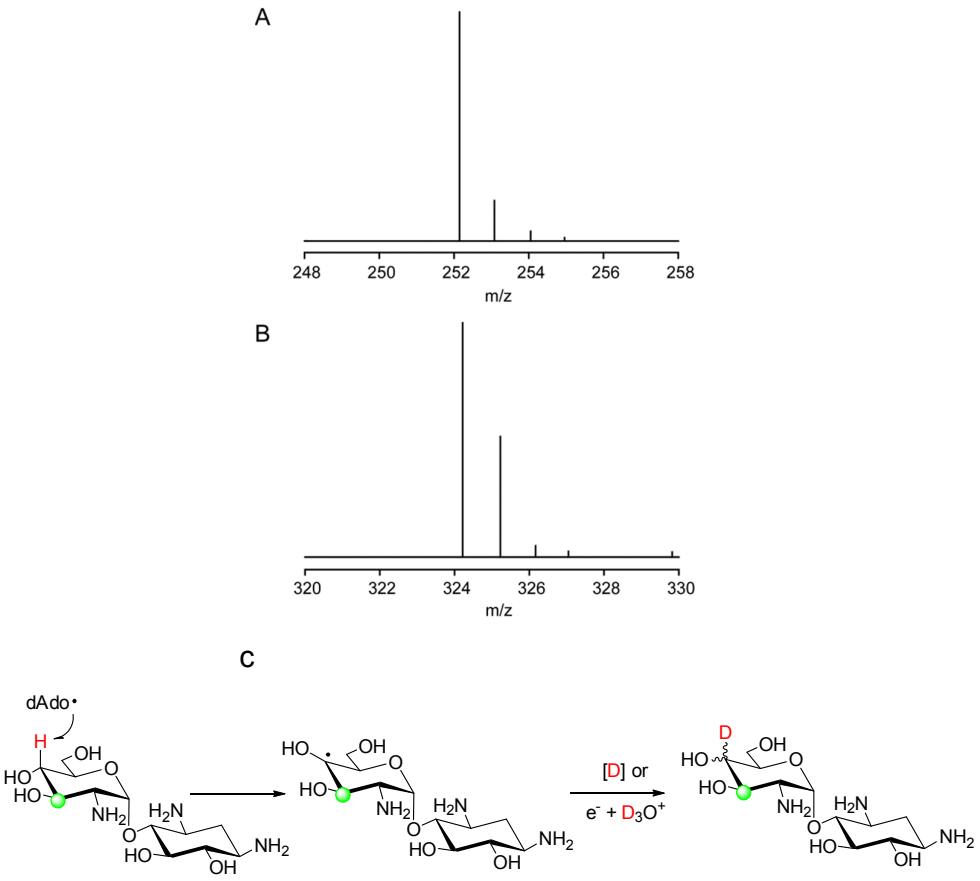

Figure S12. In-frame deletion of *aprD3* in *S. tenebrarius*, showing the schematic representation of the in-frame deletion and the southern blot analysis. The probe is shown as a purple bar, and the arrows beside the southern blot data indicate the size of the expected signal fragments.

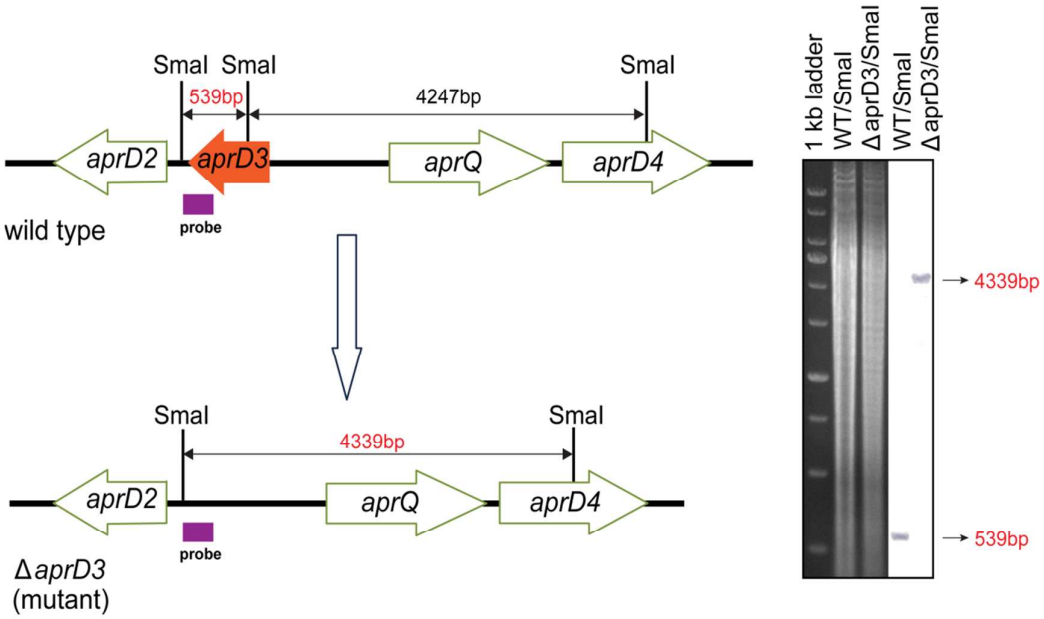

Figure S13. Structural confirmation of lividamine by using comparative MS analysis. (A) EICs of $[M + H]^+$ = 308.2 (corresponding to lividamine) for (i) reaction with AprD4 and AprD3 using paromamine as the substrate, and (ii) lividamine purified from the Δ*aprQ* mutant (also see **Figure S 14-16**). (B) MS/MS spectra of (i) the compound with $[M + H]^+$ = 308.2 from the tandem reaction catalyzed by AprD4 and AprD3 , and (ii) purified lividamine standard.

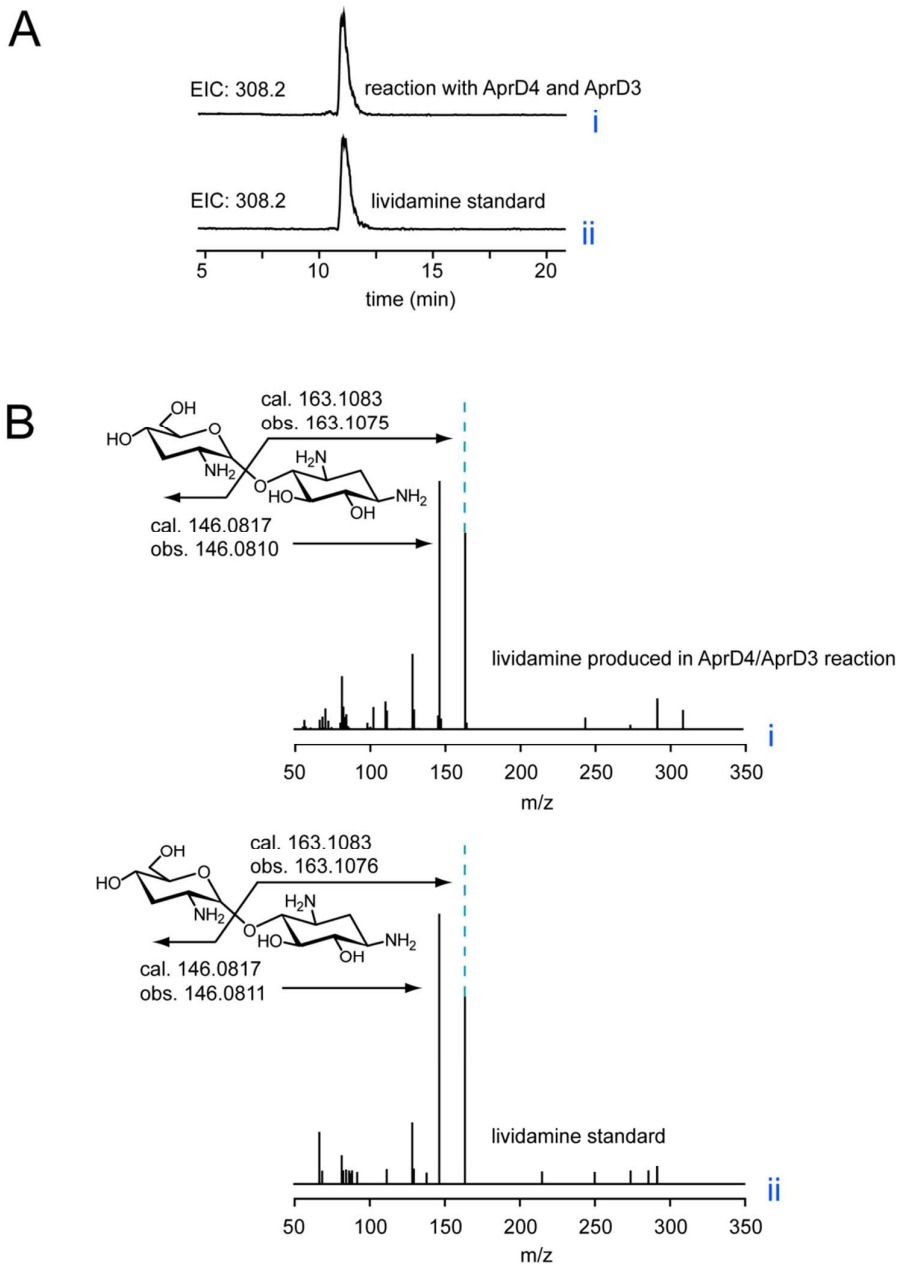

Figure S14. HR-MS/MS analysis of lividamine purified from the fermentation culture of the Δ*aprQ* mutant, showing (A) the collision induced dissociation (CID) fragments, and (B) the MS/MS spectrum.

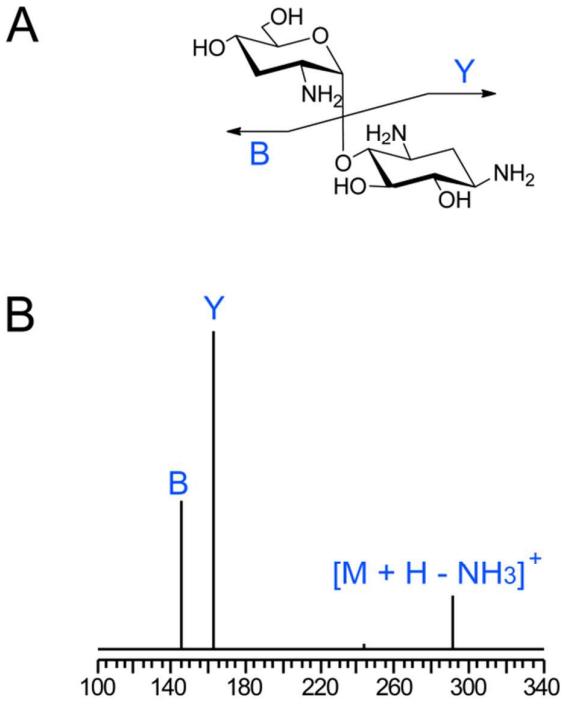

Figure S15. ^{1}H NMR analysis of lividamine purified from the fermentation culture of the Δ*aprQ* mutant, showing (A) the chemical structure of lividamine, and (B) the ^{1}H NMR spectrum.

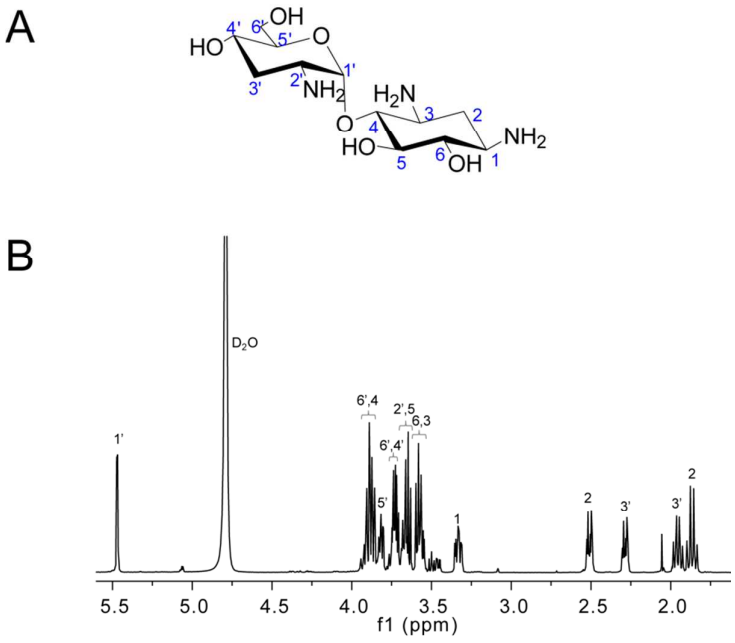

Figure S16. ^{13}C NMR analysis of lividamine purified from the fermentation culture of the Δ*aprQ* mutant, showing (A) the chemical structure of lividamine, and (B) the ^{13}C NMR spectrum.

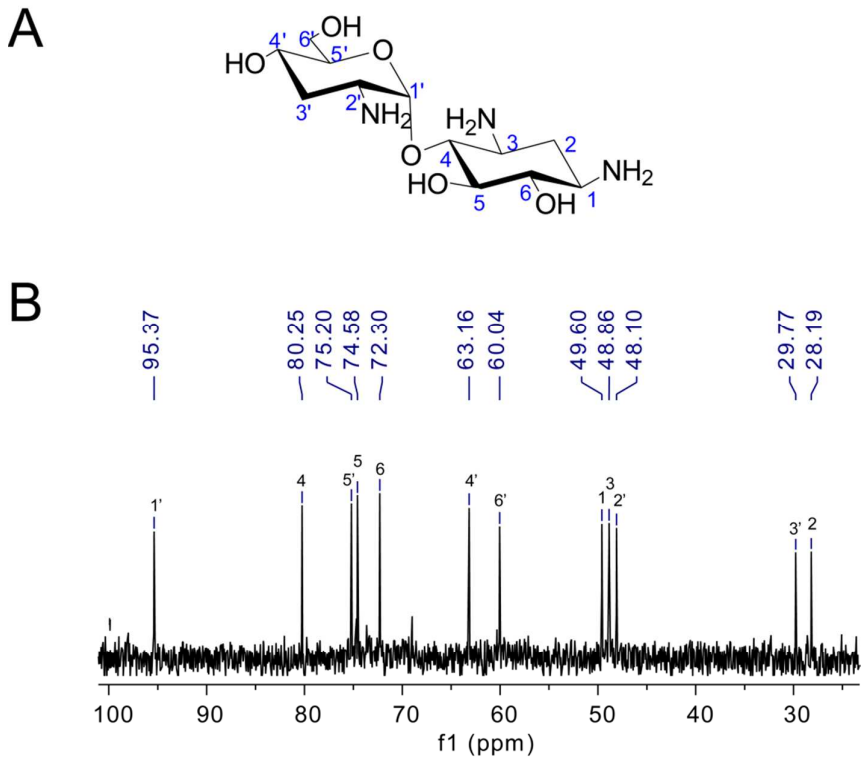

Figure S17. C3 deoxygenation involved in ascarylose biosynthesis, which is catalyzed by the coupled E1/E3 enzyme system. E1 and E3 form a catalytic complex and were co-eluted in a FPLC gel-filtration analysis.[17] Both dehydration and reduction occur at the E1 active site.

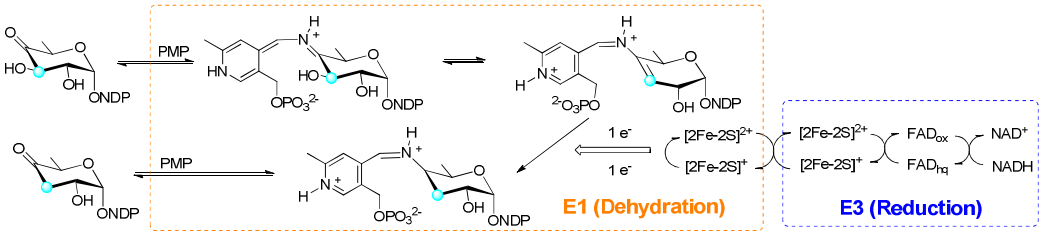

Figure S18. AprD4 and AprD3 do not form a tight protein complex. (A) SDS-PAGE analysis of purified AprD3 and AprD4. (B) Native PAGE analysis of AprD4 and AprD3 that were individually incubated or mixed together and incubated anaerobically at room temperature for 30 min or 2 h. Co-migration of AprD3 and AprD4 in the native PAGE gel was not observed in this analysis. (C) Size exclusion fast protein liquid chromatography (FPLC) analysis of AprD4 and AprD3 that were individually incubated or mixed together and incubated anaerobically at room temperature for 2 h.

A

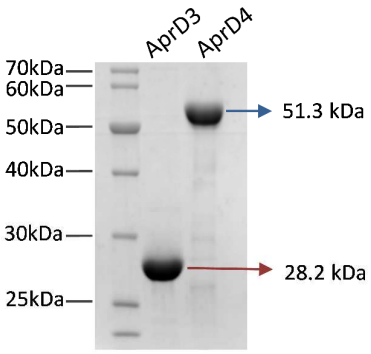

B

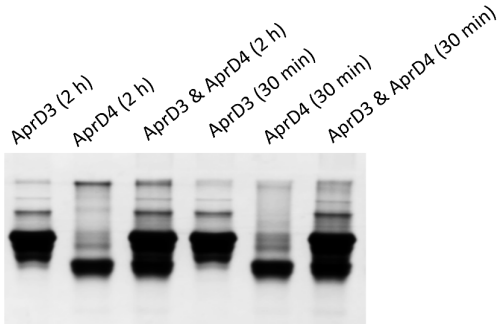

C

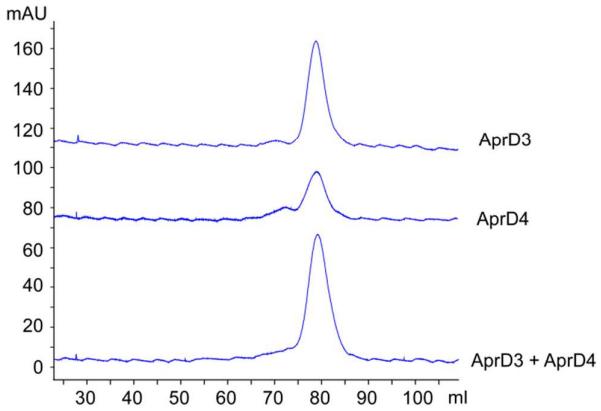

Figure S 19. Chemical structures of the representative 2-DOS-containing AGAs. The C6-amino groups or the groups derived from a C6-amino are shown in red.

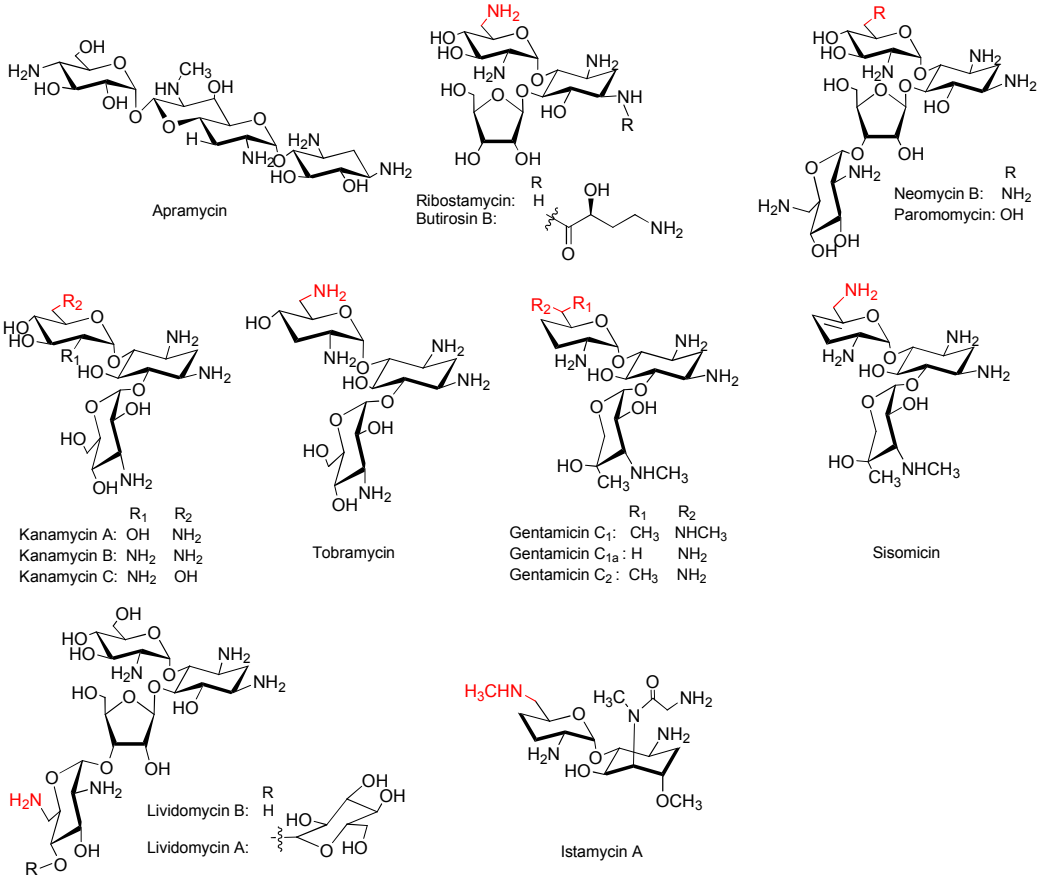

Figure S20. In-frame deletion of *aprQ* in *S. tenebrarius*, showing the schematic representation of the in-frame deletion and the southern blot analysis. The probe is shown as a purple bar, and the arrows beside the southern blot data indicate the size of the expected signal fragments.

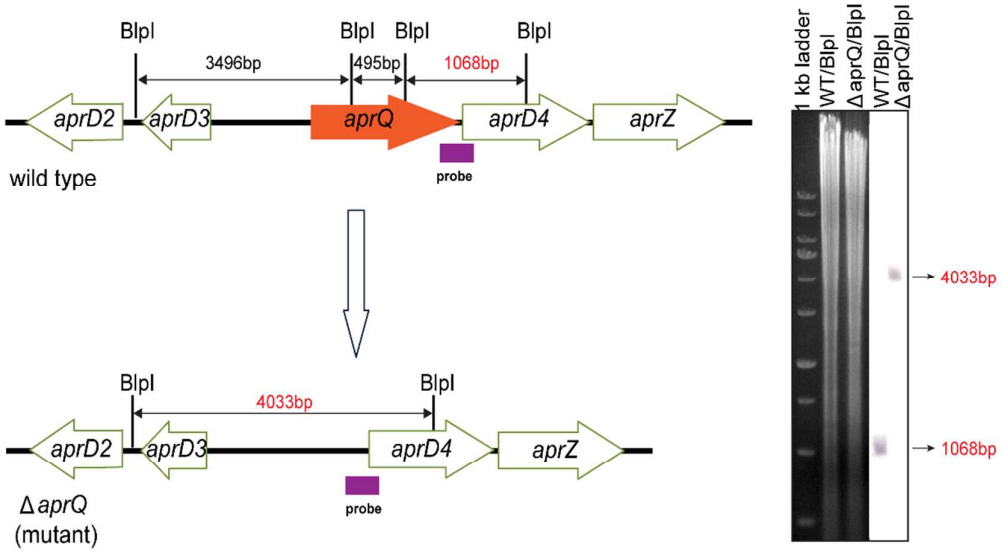

Figure S21. Generation of the *ΔaprQΔtobQ* double-knockout mutant of *S. tenebrarius*, showing the schematic representation of the in-frame deletion and the southern blot analysis. The probe is shown as a purple bar, and the arrows beside the southern blot data indicate the size of the expected signal fragments.

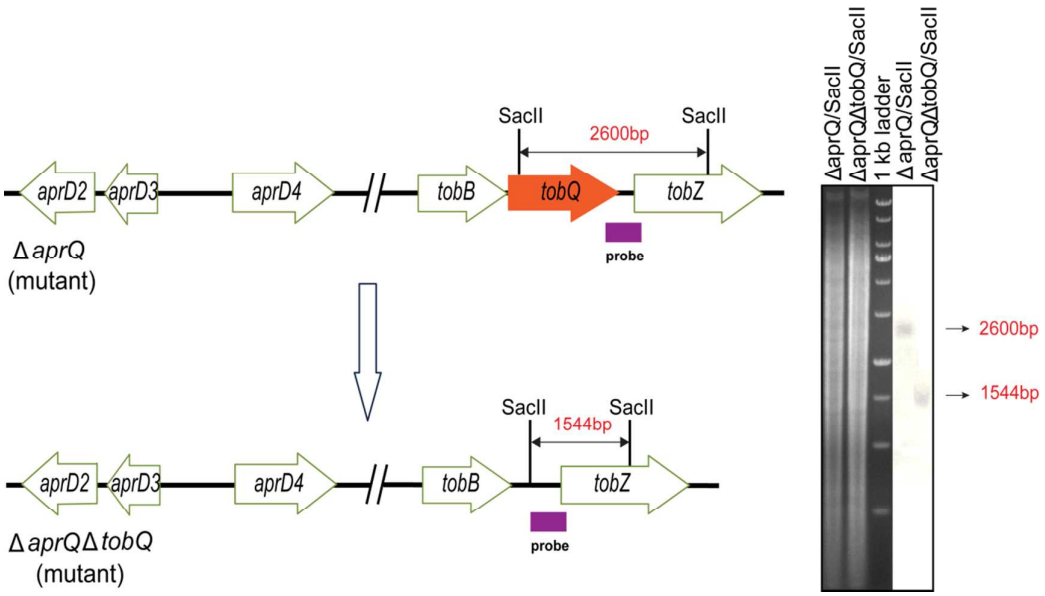

Figure S22. Generation of the *ΔaprD4ΔtobQ* double-knockout mutant of *S. tenebrarius*, showing the schematic representation of the in-frame deletion and the southern blot analysis. The probe is shown as a purple bar, and the arrows beside the southern blot data indicate the size of the expected signal fragments.

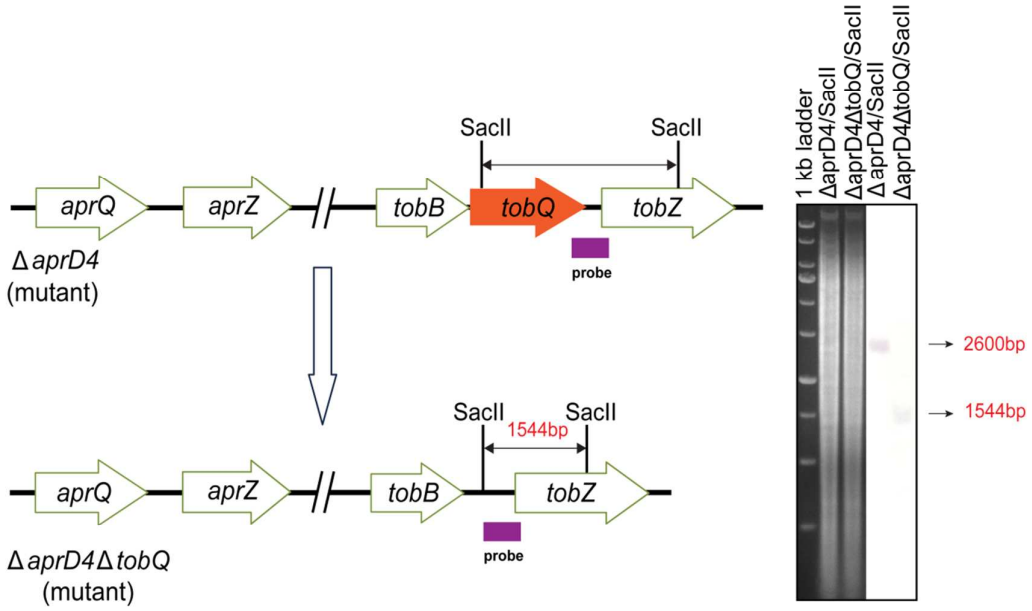

Figure S23. Generation of the*ΔaprQΔaprD4* double-knockout mutant of *S. tenebrarius*, showing the schematic representation of the in-frame deletion and the southern blot analysis. The probe is shown as a purple bar, and the arrows beside the southern blot data indicate the size of the expected signal fragments.

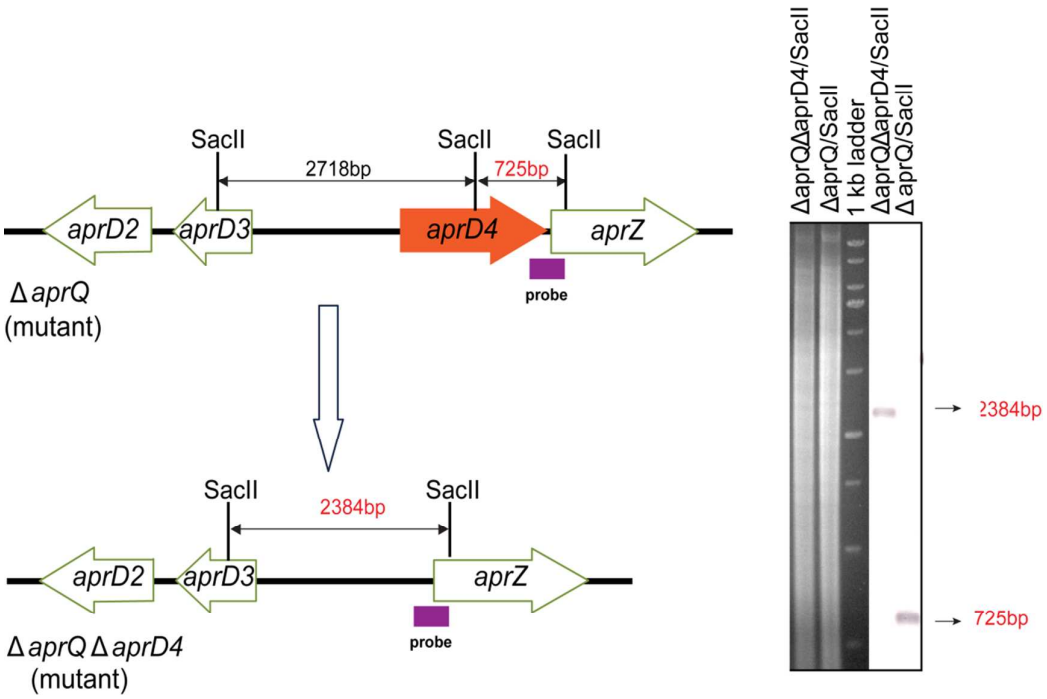

Figure S24. SDS-PAGE analysis of the purified AprQ expressed by using *Streptomyces lividans* TK24 as an expression host.

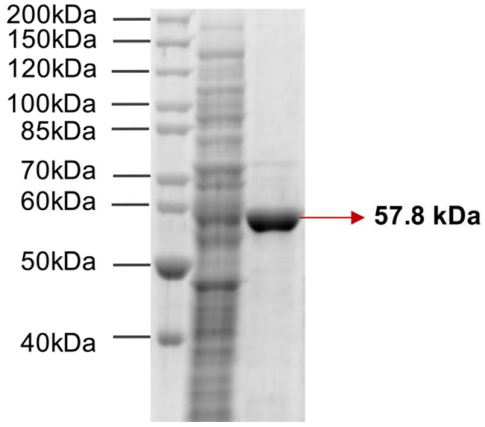

Figure S25. HR-MS/MS analysis of 6′-hydroxyl-6′-oxolividamine (HOL, **6**) generated from lividamine by AprQ.

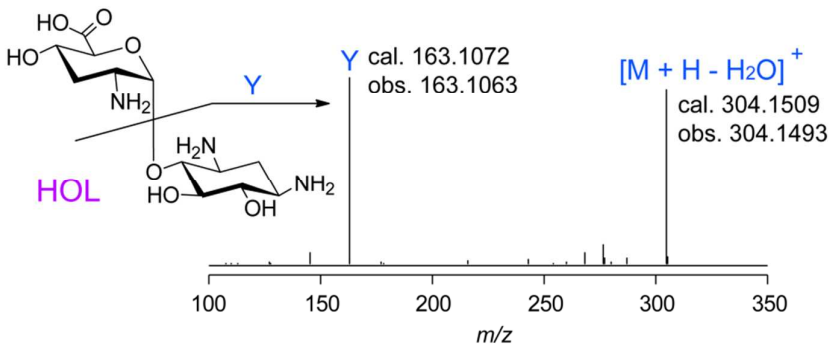

Figure S26. ^{1}H NMR analysis of 6′-hydroxyl-6′-oxolividamine (HOL, **6**) generated from lividamine by AprQ, showing (A) the chemical structure of HOL, and (B) the ^{1}H NMR spectrum.

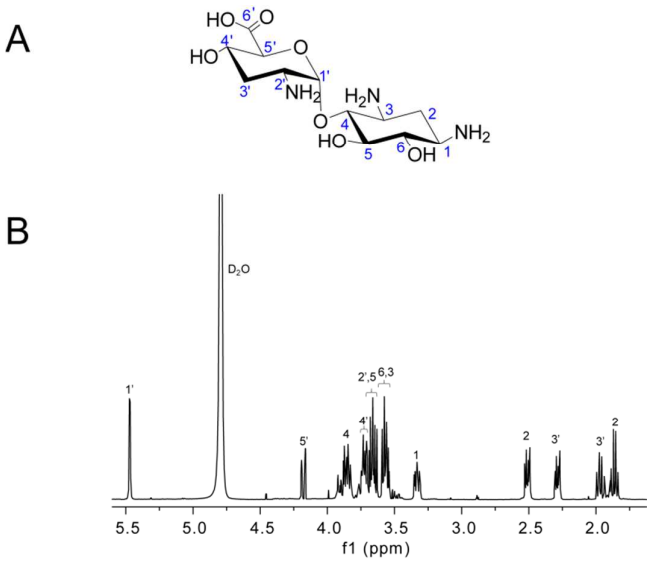

Figure S27. HR-MS/MS analysis of 6′-hydroxyl-6′-oxoparomamine (HOP, **7**) generated from paromamine by AprQ.

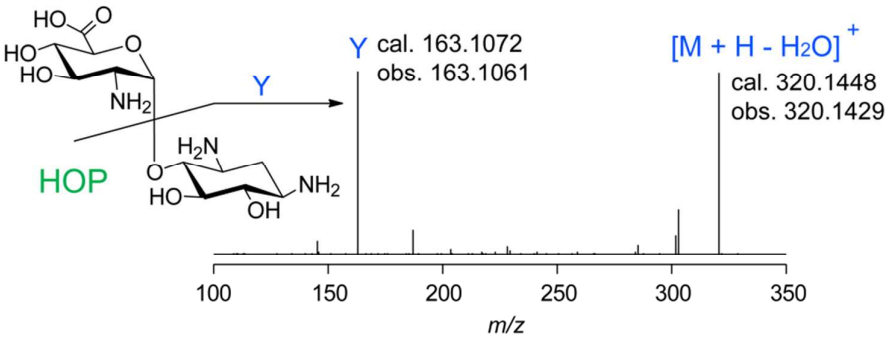

Figure S28. TobQ catalyzes the oxidation of paromamine but not lividamine. (A) LC-MS analysis of TobQ *in vitro* activity, showing the extracted ion chromatograms (EICs) of $[M + H]^+$ = 322.2 (corresponding to 6′-oxoparomamine, 6-OP) for (i) TobQ-catalyzed reaction with paromamine, and (ii) control reaction using paromamine and the boiled enzyme; and (iii) the EICs of $[M + H]^+$ = 306.2 (corresponding to 6′-oxolividamine 6-OL) for assay with lividamine and TobQ. The assay were performed using the cell free extract of *S. lividans* TK24 expressing *tobQ*. (B) TobQ converts paromamine to 6-OP. (C) TobQ was not able to convert lividamine to 6-OL. (D) HR-MS/MS characterization of 6-OP produced in the TobQ in vitro assay.

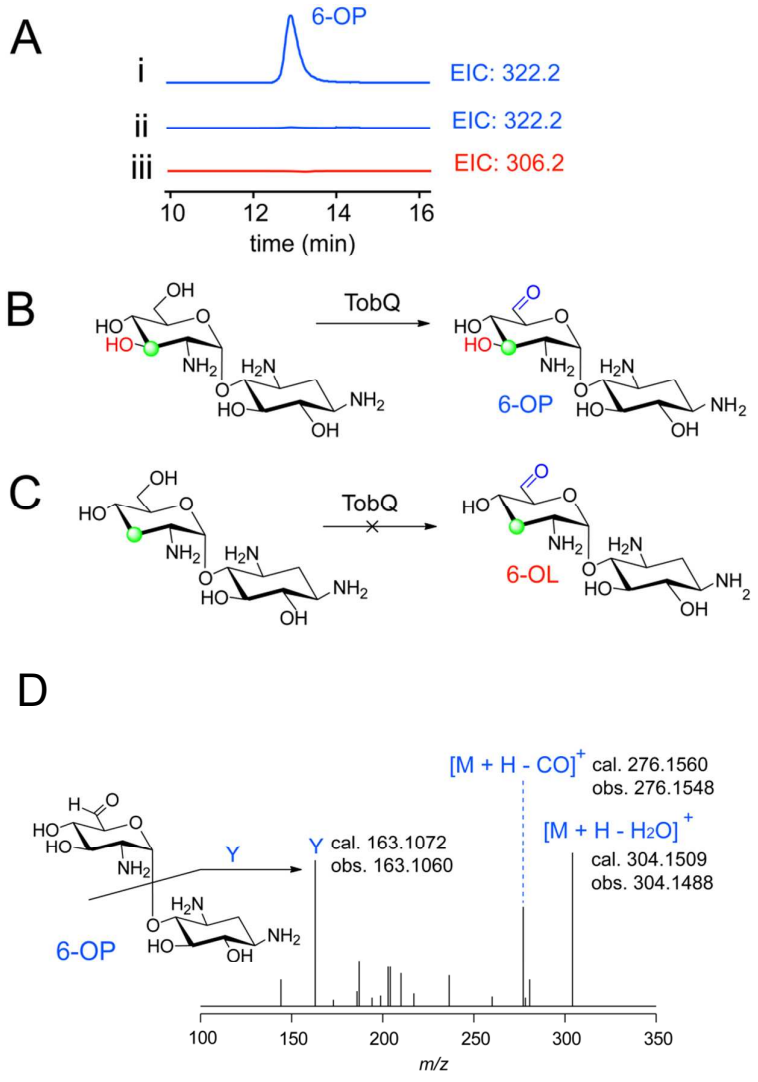

Figure S29. Unrooted Bayesian Markov chain Monte Carlo (MCMC) tree of AprQ homologous proteins. The Bayesian posterior probability (bPP) is shown along the branches, which are colored according to the taxonomies of the host organisms.

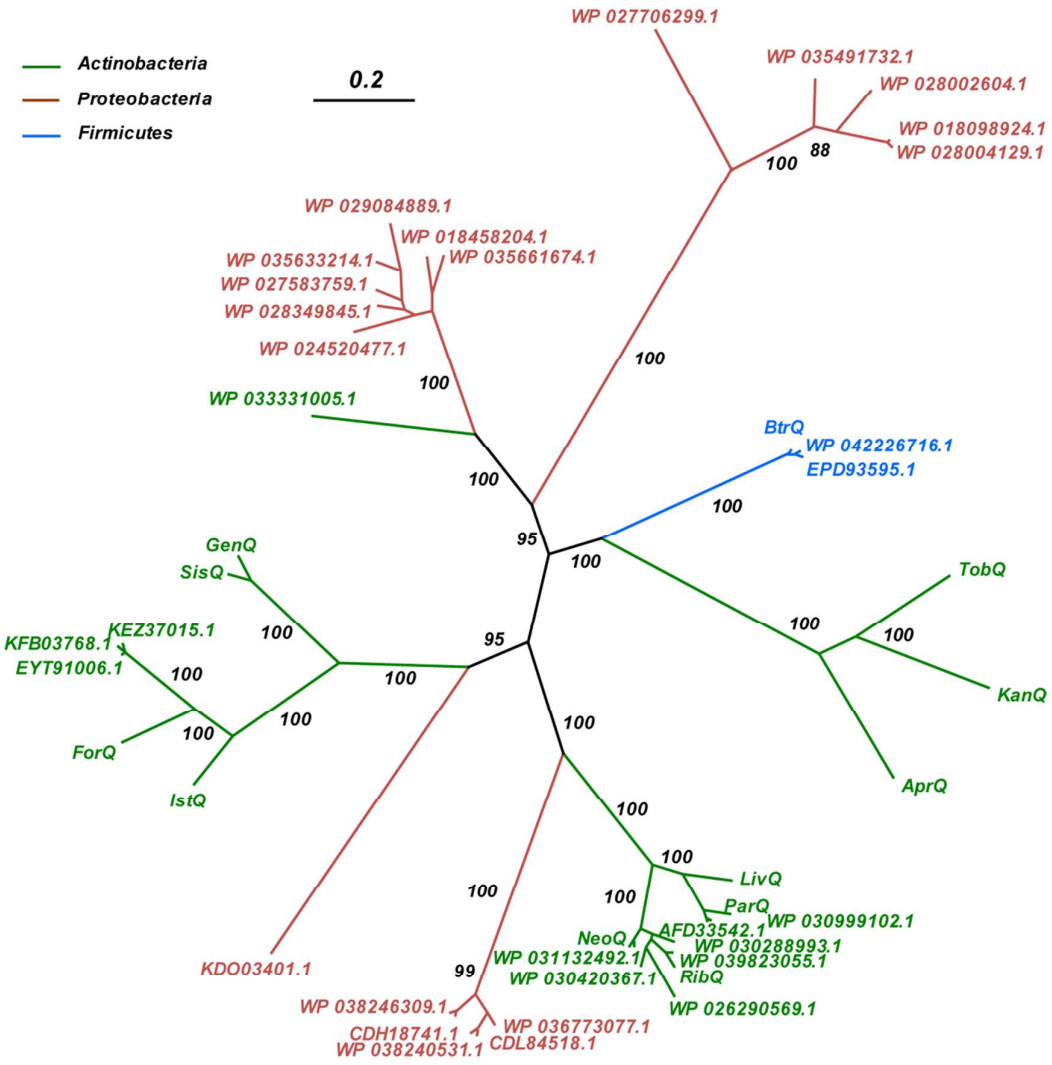

Figure S30. Summary of the GenQ in vitro activity (also see Figure S31). (A) GenQ catalyzes the oxidation of gentamicin G418 and X2. (B) GenQ is not able to catalyze the oxidation of lividamine (C) GenQ is not able to catalyze the oxidation of paromamine. 6-OL, 6′-oxolividamine; 6-OP, 6′-oxoparomamine; HOP, 6′-hydroxyl-6′-oxoparomamine; HOL, 6′-hydroxyl-6′-oxolividamine; 6-OGG, 6′-oxogentamicin G418; 6-OGX, 6′-oxogentamicin X2.

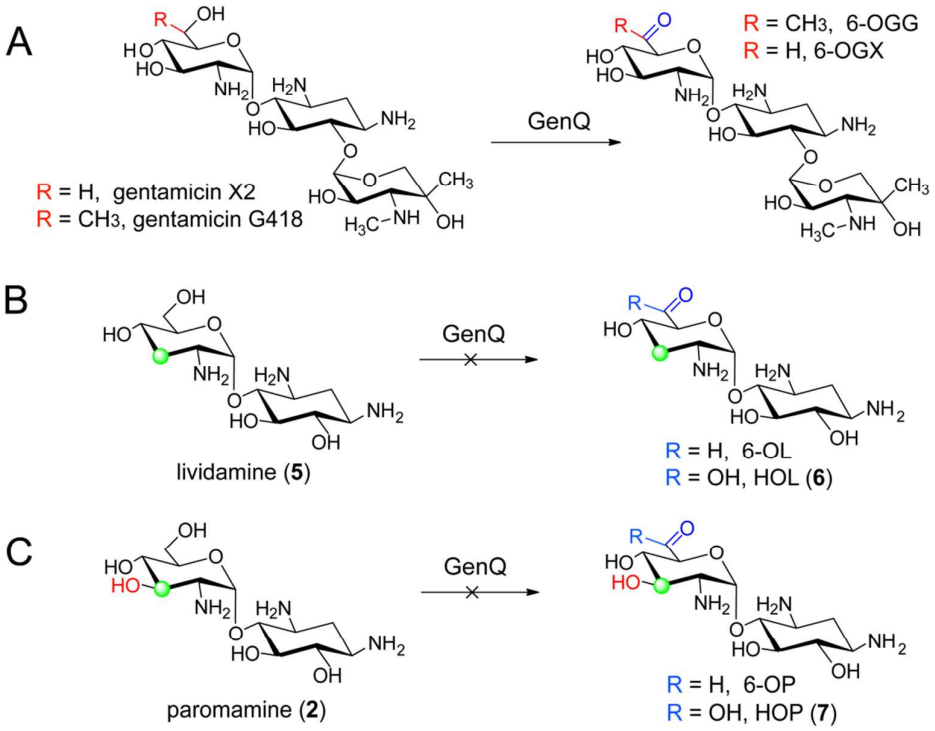

Figure S31. Biochemical study of GenQ. (A) SDS-PAGE analysis of purified GenQ. (B) LC-HR-MS analysis of GenQ in vitro assays, showing the extracted ion chromatograms (EICs) of $[M + H]^+$ = 495.3 (corresponding to 6-OGG) for (i) GenQ-catalyzed reaction with gentamicin G418, and (ii) control reaction using gentamicin G418 and boiled GenQ; and the EICs of $[M + H]^+$ = 481.3 (corresponding to 6-OGX) for (iii) GenQ-catalyzed reaction with gentamicin X2, and (iv) control reaction using gentamicin X2 and boiled GenQ; and the EICs of (v) $[M + H]^+$ = 322.2 (corresponding to 6-OP) and (vi) $[M + H]^+$ = 338.2 (corresponding to HOP) for assay containing GenQ and paromamine; and the EICs of (vii) $[M + H]^+$ = 306.2 (corresponding to 6-OL) and (viii) $[M + H]^+$ = 322.2 (corresponding to HOL) for assay containing GenQ and lividamine. 6-OL, 6′-oxolividamine; 6-OP, 6′-oxoparomamine; HOP, 6′-hydroxyl-6′-oxoparomamine; HOL, 6′-hydroxyl-6′-oxolividamine; 6-OGG, 6′-oxogentamicin G418; 6-OGX, 6′-oxogentamicin X2.

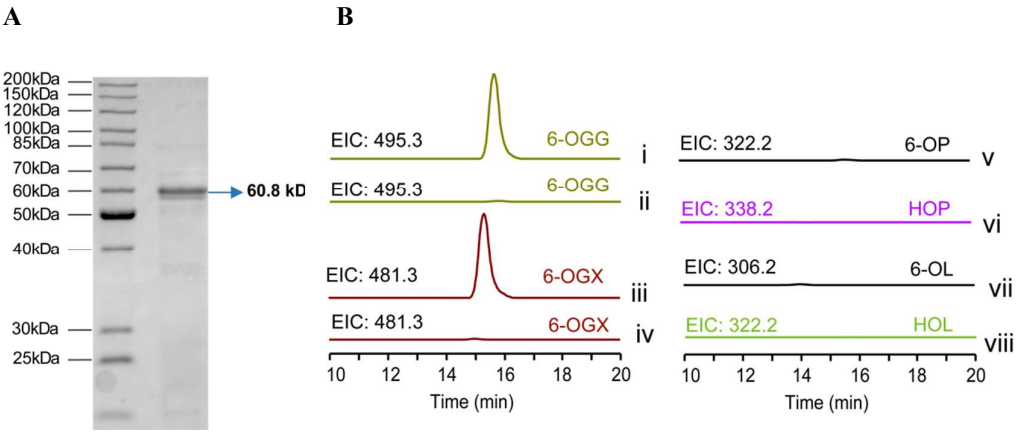

Figure S32. Comparative HR-MS/MS analysis the gentamicin analogs produced in the AprQ-catalyzed reactions, showing the spectra of 6′-hydroxyl-6′-oxogentamicin X2 **(**6-HOGX**)** and 6′-oxogentamicin G418 (6-OGG) produced in the AprQ-catalyzed reactions, and the gentamicin G418 and gentamicin X2 standards. The m/z = 163.10 signals present in all 4 spectra correspond to the protonated 2-deoxystreptamine generated upon CID-induced fragmentation.

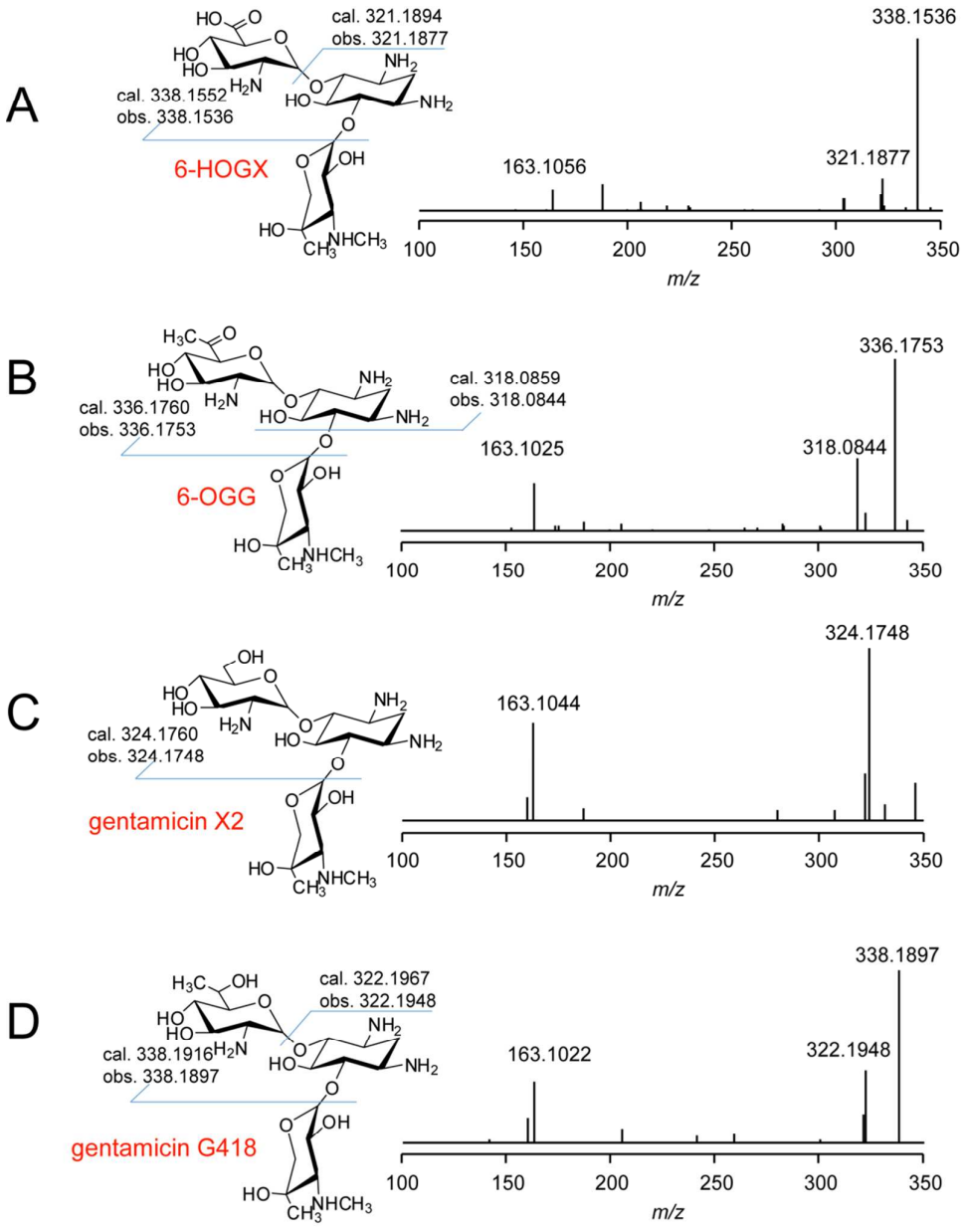

Figure S33. C3′ deoxygenation of neamine by AprD4 and AprD3. (A) EICs of $[M + H]^+$ = 307.2 (corresponding to nebramine) for (i) reaction with AprD4 and AprD3 using neamine as the substrate, (ii) control reaction using boiled AprD4 and AprD3, and (iii) synthetic nebramine standard. (B) MS/MS spectra of (i) the compound with $[M + H]^+$ = 307.2 from the tandem reaction catalyzed by AprD4 and AprD3, and (ii) synthetic nebramine standard.

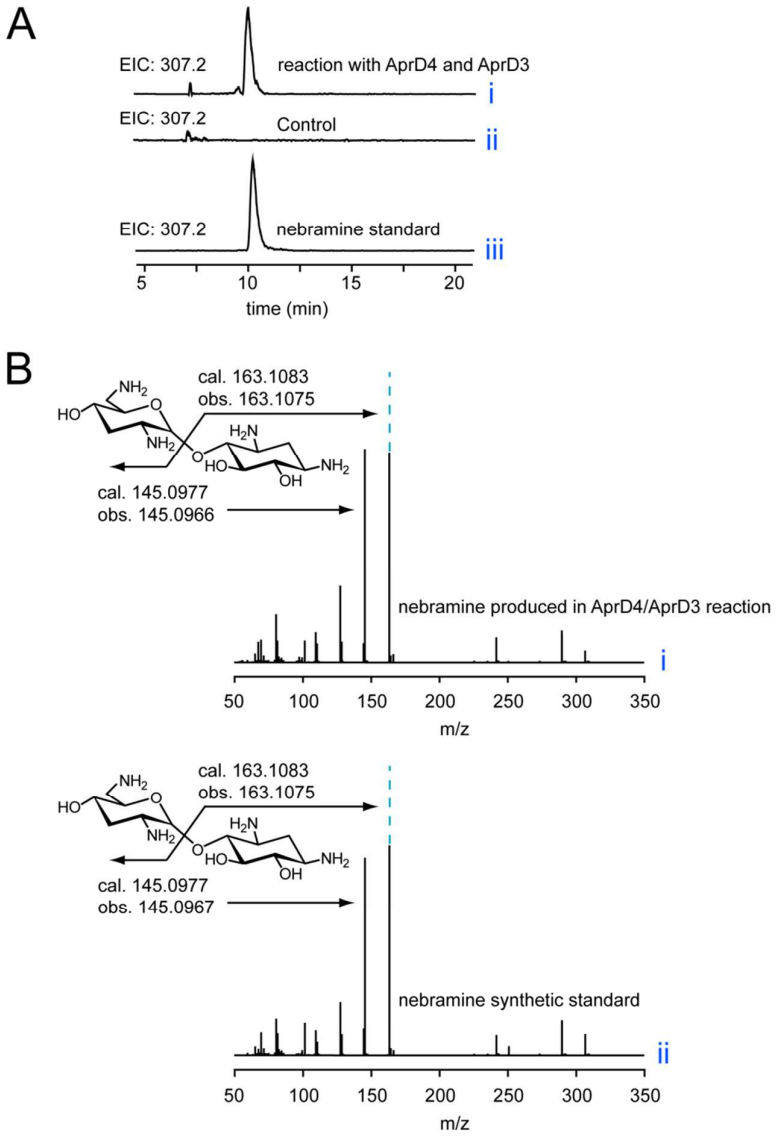

Table S1. Accession numbers of AprQ and its analogs in this study**.**

Accession Number	Bacterial strain	Taxonomy	Name/Compound
CAF33053.1	*Streptoalloteichus tenebrarius*	Actinobacteria	AprQ/apramycin
CAH18553.1	*Streptoalloteichus tenebrarius*	Actinobacteria	TobQ/tobramycin
CAF31587.1	*Streptomyces kanamyceticus*	Actinobacteria	KanQ/kanamycin
WP_042226716.1	*Paenibacillus chitinolyticus*	Firmicutes	
EPD93595.1	*Paenibacillus sp.* HGH0039	Firmicutes	
CAG77432.1	*Bacillus circulans*	Firmicutes	BtrQ/butirosin
WP_035633214.1	*Bradyrhizobium elkanii*	Proteobacteria	
CAF32378.1	*Streptomyces rimosus*	Actinobacteria	ParQ/paromomycin
WP_030999102.1	*Streptomyces sp.* NRRL WC-3773	Actinobacteria	
WP_024520477.1	*Bradyrhizobium sp.* Tv2a-2	Proteobacteria	
CAF31536.1	*Micromonospora olivasterospora*	Actinobacteria	ForQ/fortimicin
WP_018458204.1	*Bradyrhizobium sp.* WSM4349	Proteobacteria	
WP_030288993.1	*Streptomyces catenulae*	Actinobacteria	
CAG38701.1	*Streptomyces lividus*	Actinobacteria	LivQ/lividomycin
EYT91006.1	*Frankia sp.* Thr	Actinobacteria	
KFB03768.1	*Frankia sp.* Allo2	Actinobacteria	
KEZ37015.1	*Frankia sp.* CeD	Actinobacteria	
WP_027583759.1	*Bradyrhizobium sp.* Ai1a-2	Proteobacteria	
WP_033331005.1	*Actinomadura madurae*	Actinobacteria	
CDL84518.1	*Xenorhabdus szentirmaii* DSM 16338	Proteobacteria	
WP_038240531.1	*Xenorhabdus szentirmaii*	Proteobacteria	
WP_038246309.1	*Xenorhabdus bovienii*	Proteobacteria	
CDH18741.1	*Xenorhabdus bovienii*	Proteobacteria	
WP_039823055.1	*Streptomyces xinghaiensis*	Actinobacteria	
WP_026290569.1	*Streptomyces sp.* CNB091	Actinobacteria	
AFD33542.1	*Streptomyces xinghaiensis* S187	Actinobacteria	
ACN38340.1	*Micromonospora inyonensis*	Actinobacteria	SisQ/sisomicin
WP_029084889.1	*Bradyrhizobium sp.* th.b2	Proteobacteria	
WP_028349845.1	*Bradyrhizobium elkanii*	Proteobacteria	
WP_035661674.1	*Bradyrhizobium sp.* Ec3.3	Proteobacteria	
WP_030420367.1	*Streptomyces sp.* NRRL F-5065	Actinobacteria	
WP_036773077.1	*Photorhabdus asymbiotica*	Proteobacteria	
CAH60158.1	*Streptomyces tenjimariensis*	Actinobacteria	IstQ/istamycin
CAG34033.1	*Streptomyces ribosidificus*	Actinobacteria	RibQ/ribostamycin
WP_031132492.1	*Streptomyces sp.* NRRL WC-3719	Actinobacteria	
CAF31426.2	*Micromonospora echinospora*	Actinobacteria	GenQ/gentamicin
CAF33316.1	*Streptomyces fradiae*	Actinobacteria	NeoQ/neomycin
KDO03401.1	*Rickettsia buchneri*	Proteobacteria	
WP_018098924.1	*Sinorhizobium meliloti*	Proteobacteria	
WP_028004129.1	*Sinorhizobium*	Proteobacteria	
WP_028002604.1	*Sinorhizobium arboris*	Proteobacteria	
WP_035491732.1	*Burkholderia sp.* JPY251	Proteobacteria	
WP_027706299.1	*Zymobacter palmae*	Proteobacteria	

Table S2. PCR primers used in this study.

Primer	Sequence*	Function
aadA-F	CTTCGGAATAGGAACTTCATGAGCTC	*aadA* amplification
aadA-R	AACGAGCTCATACCGAAAAAATCGCTATAATGACCC	*aadA* amplification
aprD3-left-F	GGCCAGTGCCAAGCTTTCCTGGTGCTGGCCTTGGTGCTGGTGCT	*aprD3* in-frame deletion
aprD3-left-R	GTCGCGGACGTCGCGACCGACATGGGCGGTCCGGAGGCC	*aprD3* in-frame deletion
aprD3-right-F	CGCGACGTCCGCGACGTCGCGGCAGGCCAGGA	*aprD3* in-frame deletion
aprD3-right-R	ACATGATTACGAATTCAGGTAGACGCTGTTCTTCATGGCCAGGTGC	*aprD3* in-frame deletion
id-aprD3-F	TGTCACCGGTTTTCCTGGGTGCTC	WDY289 verification
id-aprD3-R	GAAGACGTGTCGGAACAGTGGAACG	WDY289 verification
HB-aprD3-F	TCGGAATTCACGACGCCGACCACCGCGGGACGGGGGGCG	*ΔaprD3* complementation
HB-aprD3-R	ACGCATATGGAGCAACGGTACGTGCTGGTCACCGGGGCC	*ΔaprD3* complementation
aprD4-left-F	GGCCAGTGCCAAGCTTCGACGTTGAGGAAACGGTATACCCGACCCG	*aprD4* in-frame deletion
aprD4aprQ-F	GGCCAGTGCCAAGCTTGGCGTCGACCACCGCCGTCACGGCCGCGTC	*aprD4aprQ* in-frame deletion
aprD4-left-R	CACCGCGATCTGGTGGCAGACCGTGCCGAGCCCGCCCGC	*aprD4/aprD4aprQ* in-frame deletion

Primer	Sequence*	Function
aprD4-right-F	CACCAGATCGCGGTGGACAAGGGGT	*aprD4/aprD4aprQ* in-frame deletion
aprD4-right-R	ACATGATTACGAATTCCAGGCCGTGGTTGCGCAGCAGCCG	*aprD4/aprD4aprQ* in-frame deletion
id-aprD4-F	TCTTCCCCTTCGCCGGCAACCTCAA	WDY288 verification
id-aprD4-R	GGTCGCCGATGCTCAGCTCGTCGGT	WDY288 verification
HB-AprD4-F	AATCATATGCGACGAATGCGGCTCGGCACGGTACTGCTG	Δ*aprD4* complementation
HB-AprD4-R	CCAGAATTCAGGCGTCACCGGTCGACCAGGCGTGCACCC	Δ*aprD4* complementation
aprQ-left-F	GGCCAGTGCCAAGCTTCGGGAGGGTTCGTGGGGAATGGGG	*aprQ* in-frame deletion
aprQ-left-R	CCGCTCGGCCAGAGTGAACGCCGTGA	*aprQ* in-frame deletion
aprQ-right-F	GACTACGACAACGTGTGGGCGGTCG	*aprQ* in-frame deletion
aprQ-right-R	ACATGATTACGAATTCCGCCGCCCATCATCACGTCGGCCC	*aprQ* in-frame deletion
id-aprQ-id-F	ACCTCCGTTCGAGTGACAATGGTC	WDY290 verification
id-aprQ-R	GCCAGGCGCATCAGGTCGAGCGGG	WDY290 verification
HB-aprQ-F	GTAGGATCCACATATGAGGTTCGTGACGCTCCAGGAGGCCACC	*ΔaprQ* complementation
HB-aprQ-R	GACATGATTACGAATTCGGAACCGGGGGTGTCAGGAGATGGCG	*ΔaprQ* complementation
tobQ-left-F	GGCCAGTGCCAAGCTTGACTCTGTCGCCGGCCGTGATGTGTCCAC	*tobQ* in-frame deletion
tobQ-left-R	CAAGGCAGGGGCGATCGACGTGCGGGAGGTGGACA	*tobQ* in-frame deletion
tobQ-right-F	ATCGCCCCTGCCTTGCCGTCGCGCGTCCACCGCCCGTGGCGACGC	*tobQ* in-frame deletion

Primer	Sequence*	Function
tobQ-right-R	ACATGATTACGAATTCGCACAGCATGACGGCGATCGACGAGTAC	*tobQ* in-frame deletion
id-tobQ-F	CCGCCTGCACCGGGGCCGTGTTGTAC	WDY291 and WDY292 verification
id-tobQ-R	CCCTGCTGCGGCACGGCGTCTTCTG	Same to id-tobQ-F
HB-tobQ-F	GTAGGATCCACATATGCTGCTGATCTCAGCGGACGAGGCCGCGC	*ΔtobQ* complementation
HB-tobQ-R	GACATGATTACGAATTCGGAACCGGTGTGAGGAACCGGTGTGGC	*ΔtobQ* complementation
pGM1190_F	AGAGAAGGGAGCGGACCATGGGCAGCAGCCATCATCATCATCATC	pWDYHS01 construction
pGM1190_R	AAACTTTAGATCTGGGTTAGCAGCCGGATCTCAGTGGTGG	pWDYHS01 construction
N-AprD3-F	AAGGAGATATACCATGGGCCATCATCATCATCATCACATGGAGCAACGGTACGTGCTGG	AprD3 overexpression (His-Tagged)
N-AprD3-R	GGTGGTGGTGCTCGAGTTATTATCACGACGCCGACCACCGCGGGAC	AprD3 overexpression (His-Tagged)
N-AprD4-F	AAGGAGATATACCATGGGCCATCATCATCATCATCACGTGAATGAGGTGCGACGAATGC	AprD4 overexpression
N-AprD4-R	GGTGGTGGTGCTCGAGTTATTATCAGGCGTCACCGGTCGACCAGGC	AprD4 overexpression
N-flag-AprD3-F	ATACCATGGGCGACTACAAGGACGACGATGACAAAATGGAGCAACGGTACGTGCTGGTC	AprD3 overexpression (Flag-Tagged)
N-AprQ-F	GCGCGGCAGCCATATGATGAGGTTCGTGACGCTCCAGGAGGCCACC	AprQ overexpression
N-AprQ-R	GGTGGTGGTGCTCGAGTTATTATCAGGAGATGGCGCAGGCGATCCG	AprQ overexpression
N-TobQ-F	AGGCATATGCTGCTGATCTCAGCGGACGAGGCCGC	TobQ overexpression
N-TobQ-R	GGTGGTGGTGCTCGAGTTATTATCAGTCGATCGCGGACGCGATCCG	TobQ overexpression
AprD4 C203A-F	CGGCAGCTTCGGCGCCCCCTACCCGTGCC	AprD4 mutagenesis
AprD4	GGCACGGGTAGGGGGCGCCGAAGCTGCCG	AprD4

Primer	Sequence*	Function
C203A-R		mutagenesis
AprD4 C207A-F	CTGCCCCTACCCGGCCCGCTTCTACTGCC	AprD4 mutagenesis
AprD4 C207A-R	GGCAGTAGAAGCGGGCCGGGTAGGGGCAG	AprD4 mutagenesis
AprD4 C211A-F	CGTGCCGCTTCTACGCCCCGTACCCGCTC	AprD4 mutagenesis
AprD4 C211A-R	GAGCGGGTACGGGGCGTAGAAGCGGCACG	AprD4 mutagenesis
AprD4 C31A-F	GGGCTCGGCACGGTCGCCAAGGACGAGGACTTC	AprD4 mutagenesis
AprD4 C31A-R	GAAGTCCTCGTCCTTGGCGACCGTGCCGAGCCC	AprD4 mutagenesis
AprD4 C79A-F	GGCACCACGGTGATCGCCCACGTCTCGCTGCC	AprD4 mutagenesis
AprD4 C79A-R	GGCAGCGAGACGTGGGCGATCACCGTGGTGCC	AprD4 mutagenesis
AprD4 C103A-F	CGCAGGGCGCCCGCGCCTACGCCTACACG	AprD4 mutagenesis
AprD4 C103A-R	CGTGTAGGCGTAGGCGCGGGCGCCCTGCG	AprD4 mutagenesis
AprD4 C124A-F	GAGCGGGGCGGCGCCGAGGGCGTCCTG	AprD4 mutagenesis
AprD4 C124A-R	CAGGACGCCCTCGGCGCCGCCCCGCTC	AprD4 mutagenesis
AprD4 C236A-F	CGGAGTTCCGGCAGGCCGCCGAGCTGGGC	AprD4 mutagenesis
AprD4 C236A-R	GCCCAGCTCGGCGGCCTGCCGGAACTCCG	AprD4 mutagenesis
AprD4 C262A-F	CGCACCCTGGAGCTGGCCCAGGCCCTCAAGG	AprD4 mutagenesis
AprD4 C262A-R	CCTTGAGGGCCTGGGCCAGCTCCAGGGTGCG	AprD4 mutagenesis
AprD4 C276A-F	GGGTGCCCTGGTGGGCCGAGACCCGGATCG	AprD4 mutagenesis
AprD4 C276A-R	CGATCCGGGTCTCGGCCCACCAGGGCACCC	AprD4 mutagenesis
AprD4 C296A-F	GGTCGACGCCGGGGCCGTCGGCGTCGAG	AprD4 mutagenesis
AprD4 C296A-R	CTCGACGCCGACGGCCCCGGCGTCGACC	AprD4 mutagenesis

Primer	Sequence*	Function
AprD4 C432A-F	GCTGCACGCGGTCGCCAAGGCGGGGCCC	AprD4 mutagenesis
AprD4 C432A-R	GGGCCCCGCCTTGGCGACCGCGTGCAGC	AprD4 mutagenesis

*Restriction sites are underlined.

Table S3. Plasmids (for *Streptomyces* genetics) and *Streptomyces* strains used in this study.

Strain/plasmid	Relevant genotype/comments
Plasmids	
pWHU258	*aac(3)IV* was replaced by *aadA* in pOJ260
pWHU268	*aac(3)IV* was replaced by *aadA* in pIB139
pWDYHS01	His_6-tag was inserted downstream of tipA promoter in protein overexpression vector in Streptomyces (tsr, *aphII*, PtipA promoter, RBS, N/C-terminal His_6-tag, fd terminator)
pWHU288	*aprD4* in-frame deletion construction
pWHU289	*aprD3* in-frame deletion construction
pWHU290	*aprQ* in-frame deletion construction
pWHU291	*tobQ* in-frame deletion construction
pWHU293	*aprD4aprQ* double in-frame deletion construction
pWHU300	*aprD4* complementation construction
pWHU301	*aprD3* complementation construction
pWHU302	*aprQ* complementation construction
pWHU303	*tobQ* complementation construction
pWHU320	AprQ overexpression construction
pWHU321	TobQ overexpression construction
Streptomyces	
S. tenebrarius	apramycin producer strain
WDY288	*aprD4* in-frame deletion mutant
WDY289	*aprD3* in-frame deletion mutant
WDY290	*aprQ* in-frame deletion mutant
WDY291	*tobQ* in-frame deletion mutant
WDY292	*aprQ tobQ* double in-frame deletion mutant
WDY293	*aprD4 aprQ* double in-frame deletion mutant
WDY294	*aprD4 tobQ* double in-frame deletion mutant
WDY300	*aprD4* complementation mutant
WDY301	*aprD3* complementation mutant
WDY302	*aprQ* complementation mutant
WDY303	*tobQ* complementation mutant
WDY306	*aprQ* complemented to WDY292 mutant
WDY307	*aprQ* complemented to WDY293 mutant
WDY308	*tobQ* complemented to WDY293 mutant
WDY320	AprQ overexpression in *S. lividans* TK24
WDY321	TobQ overexpression in *S. lividans* TK24

References

(1) Guo, J.; Huang, F.; Huang, C.; Duan, X.; Jian, X.; Leeper, F.; Deng, Z.; Leadlay, P. F.; Sun, Y. *Chem Biol* **2014**, *21*, 608.

(2) Li, R.; Zhu, H.; Ruan, J.; Qian, W.; Fang, X.; Shi, Z.; Li, Y.; Li, S.; Shan, G.; Kristiansen, K.; Yang, H.; Wang, J. *Genome Res.* **2010**, *20*, 265.

(3) Gust, B.; Challis, G. L.; Fowler, K.; Kieser, T.; Chater, K. F. *Proc Natl Acad Sci U S A* **2003**, *100*, 1541.

(4) Bierman, M.; Logan, R.; O'Brien, K.; Seno, E. T.; Rao, R. N.; Schoner, B. E. *Gene* **1992**, *116*, 43.

(5) Wilkinson, C. J.; Hughes-Thomas, Z. A.; Martin, C. J.; Bohm, I.; Mironenko, T.; Deacon, M.; Wheatcroft, M.; Wirtz, G.; Staunton, J.; Leadlay, P. F. *J Mol Microbiol Biotechnol* **2002**, *4*, 417.

(6) Kieser, T.; Bibb, M. J.; Buttner, M. J.; Chater, K. F.; Hopwood, D. A. *Practical Streptomyces genetics* **2000**, *The John Innes Foundation*.

(7) Thorpe, H. M.; Smith, M. C. *Proc Natl Acad Sci U S A* **1998**, *95*, 5505.

(8) Combes, P.; Till, R.; Bee, S.; Smith, M. C. *J Bacteriol* **2002**, *184*, 5746.

(9) Zheng, L.; Baumann, U.; Reymond, J. L. *Nucleic Acids Research* **2004**, *32*.

(10) Muth, G.; Nussbaumer, B.; Wohlleben, W.; Puhler, A. *Mol Gen Genet* **1989**, *219*, 341.

(11) Thompson, J. D.; Gibson, T. J.; Plewniak, F.; Jeanmougin, F.; Higgins, D. G. *Nucleic Acids Res* **1997**, *25*, 4876.

(12) Ronquist, F.; Teslenko, M.; van der Mark, P.; Ayres, D. L.; Darling, A.; Hohna, S.; Larget, B.; Liu, L.; Suchard, M. A.; Huelsenbeck, J. P. *Syst Biol* **2012**, *61*, 539.

(13) Page, R. D. *Comput Appl Biosci* **1996**, *12*, 357.

(14) Ko, Y.; Ruszczycky, M. W.; Choi, S. H.; Liu, H. W. *Angew Chem Int Ed Engl* **2015**, *54*, 860.

(15) Lin, G. M.; Choi, S. H.; Ruszczycky, M. W.; Liu, H. W. *J Am Chem Soc* **2015**, *137*, 4964.

(16) Ji, X. J.; Li, Y. Z.; Jia, Y. L.; Ding, W.; Zhang, Q. *Angew Chem Int Edit* **2016**, *55*, 3334.

(17) Chen, X. M. H.; Ploux, O.; Liu, H. W. *Biochemistry* **1996**, *35*, 16412.